ChemMedChem

Minireviews
doi.org/10.1002/cmdc.202100332

Chemistry
Europe
European Chemical
Societies Publishing

Special Collection

Chemical and Structural Strategies to Selectively Target mTOR Kinase

Chiara Borsari,*[a] Martina De Pascale,[a] and Matthias P. Wymann[a]

Dysregulation of the mechanistic target of rapamycin (mTOR) pathway is implicated in cancer and neurological disorder, which identifies mTOR inhibition as promising strategy for the treatment of a variety of human disorders. First-generation mTOR inhibitors include rapamycin and its analogues (rapalogs) which act as allosteric inhibitors of TORC1. Structurally unrelated, ATP-competitive inhibitors that directly target the mTOR catalytic site inhibit both TORC1 and TORC2. Here, we review investigations of chemical scaffolds explored for the development of highly selective ATP-competitive mTOR kinase inhibitors (TORKi). Extensive medicinal chemistry campaigns allowed to overcome challenges related to structural similarity between mTOR and the phosphoinositide 3-kinase (PI3K) family. A broad region of chemical space is covered by TORKi. Here, the investigation of chemical substitutions and physicochemical properties has shed light on the compounds' ability to cross the blood brain barrier (BBB). This work provides insights supporting the optimization of TORKi for the treatment of cancer and central nervous system disorders.

1. Introduction

Mechanistic target of rapamycin (mTOR) is an evolutionary highly conserved Serine/Threonine (Ser/Thr) protein kinase and belongs to the phosphatidylinositol 3-kinase-related kinase (PIKK) family. The mTOR kinase catalytic subunit forms two functionally distinct multi-protein complexes, mTOR complex 1 (TORC1) and mTOR complex 2 (TORC2), which are distinguished by unique accessory proteins, Raptor and Rictor, respectively.[1] TORC1 relays upstream signal input from cellular energy and stress, oxygen, amino acids, nutrients and growth factors. Activation of phosphoinositide 3-kinase (PI3K) through cell surface receptors stimulates the production of phosphatidylino-sitol(3,4,5)-trisphosphate [PtdIns(3,4,5)P_3 or PIP_3] production, which recruits protein kinase B (PKB/Akt) via its pleckstrin homology (PH) domain to the plasma membrane. Activated PKB/Akt phosphorylates Tuberin protein (TSC2), thus impairing TSC2-GAP activity and promoting TORC1 activation.[2] TORC1 regulates lipid and protein synthesis through phosphorylation of S6 kinase (S6K).[3] Moreover, TORC1 modulates lysosome function and inhibits autophagy. Less is known regarding the regulation of TORC2 activity, as compared to TORC1. It has been suggested that SIN1, a component of mTOR complex 2, plays a key role in the regulation of TORC2. PIP_3 is recognized by SIN1's PH domain, which relieves the SIN1-mediated inhibition of TORC2. Activated, the TORC2 Rictor-mTORK complex phosphorylates PKB/Akt on Ser473, which facilitates Thr308 phosphorylation by PDK1.[4] TORC2 controls cytoskeletal rearrangements, cell cycle progression, and survival.[2a]

Aberrant mTOR signaling is involved in cancer,[5] metabolic disease such as type 2 diabetes and obesity,[6] autoimmune disease,[7] rare diseases including lymphangioleiomyomatosis (LAM) and tuberous sclerosis (TSC),[8] and during aging.[9] Considering its central role in autophagy, mTOR is implicated in neurodegenerative disorders, namely Huntington's,[10] Alzheimer's,[11] and Parkinson's diseases.[12] mTOR kinase contains a number of distinct functional domains including (i) multiple Huntingtin Elongation factor 3A subunit of PP2A and TOR1 (HEAT) motifs in the N-terminal region, (ii) FRAP/TOR, ATM, TRRAP (FAT) domain, (iii) FKBP12/FPR1-rapamycin binding (FRB) domain, (iv) kinase domain and (v) a C-terminal small FAT domain (FATC) domain (Figure 1a and 1b).[13] First generation mTOR inhibitors include rapamycin and its analogues, so-called rapalogs, which are allosteric inhibitors of mTORC1: they interact simultaneously with the FRB domain of TORC1 (green in Figure 1a) and the FK506-binding protein 12 (FKBP12).[14] Since suppression of TORC1 signaling by rapamycin/rapalogs often leads to upregulation of upstream signaling limiting clinical success,[15] ATP-competitive mTOR kinase inhibitors (TORKi), targeting the function of both TORC1 and TORC2, have been developed. The development of highly selective TORKi is, however, an ongoing challenge due to the structural similarity between the catalytic sites of mTOR and phosphoinositide 3-kinases (PI3Ks, Figure 1c and 1d). The chemical structures of PI3K and mTOR inhibitors have been recently reviewed.[16] Herein, we outline a structural comparison of dual PI3K/mTOR and selective mTOR inhibitors, and we pinpoint the structural activity relationship (SAR) studies and chemical features leading to selective mTOR inhibition. Moreover, we analyze the

[a] Dr. C. Borsari, Dr. M. De Pascale, Prof. M. P. Wymann
Department of Biomedicine
University of Basel
Mattenstrasse 28
4058 Basel (Switzerland)
E-mail: chiara.borsari@unibas.ch

ChemMedChem

Minireviews
doi.org/10.1002/cmdc.202100332

Chemistry Europe
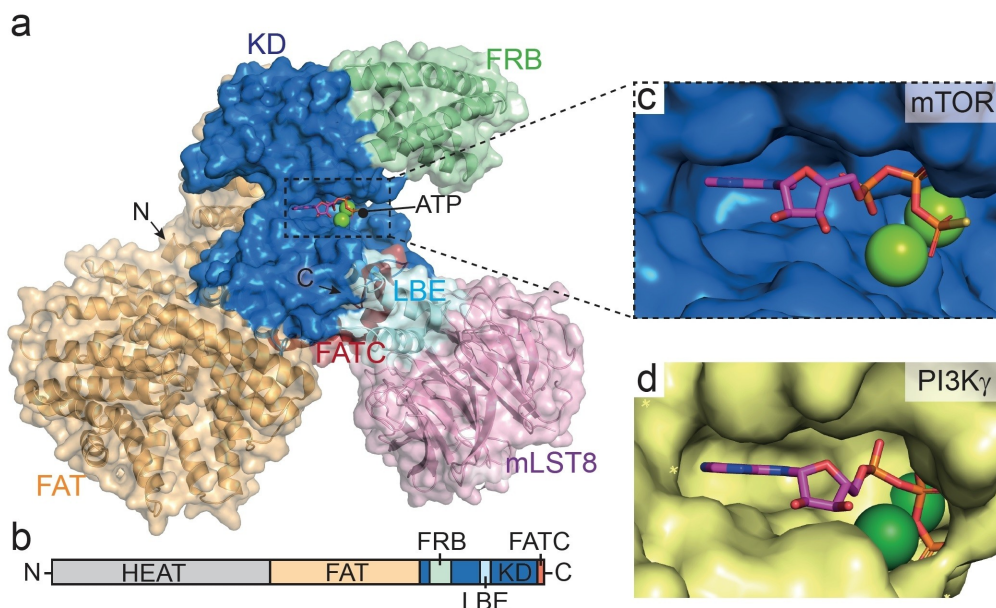European Chemical
Societies Publishing

Figure 1. a) X-ray crystallographic structure of mTOR derived from the mTOR$^{\Delta N}$-mLST8-ATPγS-Mg complex (PDB ID: 4JSP).[1b] mTOR is colored as follows: LBE (cyan), located at the C lobe, forms the binding site for mLST8 (pink). ATPγS is displayed as sticks and Mg^{2+} ions as spheres. KD (blue): kinase domain. b) Schematic representation of the domain organization of TOR. (c, d) Comparison of ATP-binding site of mTOR (c) and PI3Kγ (d). PI3Kγ (yellow) – ATP complex from PDB ID: 1E8X.[17] While the protein used in mTOR$^{\Delta N}$-mLST8-ATPγS-Mg complex is from Homo sapiens, the PI3Kγ-ATP complex is from Sus scrofa. There are, however, no expected structural and functional differences between human and pig enzymes, as the two species show complete amino acid sequence identity in the ATP site (overall sequence identity 95.3%).

Dr. Chiara Borsari, Ph.D., is a postdoctoral fellow at the Department of Biomedicine (DBM) of the University of Basel (CH). Her research focuses on the design and synthesis of small-molecule reversible and covalent anticancer agents and chemical probes targeting the PI3K-mTOR signalling pathway. After research visits at the NHRF in Athens (GR) and the State University of New York at Albany (USA), she obtained her Ph.D. from the University of Modena and Reggio Emilia (Italy) in 2017. She is a board member of the EFMC-YSN (European Federation of Medicinal Chemistry and Chemical Biology - Young Scientists Network) and the EFMC Communication Team.

Dr. Martina De Pascale, Ph.D., joined the research group of Prof. Wymann at the DBM, University of Basel (CH), in 2019 as a postdoctoral fellow. Her research is dealing with the design and synthesis of small molecules for the treatment of CNS disorders. She completed her PhD at the CERMN (Centre d'Etudes et de Recherche sur le Médicament de Normandie) in Caen (FR) working on the development of protein-protein interaction (PPIs) inhibitors as anticancer agents. During the PhD studies, she joined the University of Montreal (CA) where she expanded her knowledge to peptidomimetics.

Prof. Matthias P. Wymann, Ph.D., is at the DBM of the University of Basel (CH). He graduated from the Theodor Kocher Institute in Berne in 1988, followed by post-doctoral studies at the Institute of Microbiology in Linköping (SE), and started his independent research group at the University of Fribourg (CH) in 1991. In 2004, he was appointed to his current position. He discovered the first PI3K inhibitor, wortmannin, elucidated its covalent PI3K interactions, and investigated the role PI3K isoforms in cancer and immunity. He initiated EU framework programs (ACID) and the ESF program Euromembranes (TraPPs). He is co-founder of PIQUR Therapeutics AG, and served as consultant for different PI3K drug programs at Onyx/Parke-Davis, Ares-Serono, Novartis Horsham and Novartis Oncology Basel.

ChemMedChem

Minireviews
doi.org/10.1002/cmdc.202100332

Chemistry
Europe
European Chemical
Societies Publishing

physicochemical properties of the discussed compounds and their effects on blood-brain-barrier (BBB) permeability.

2. Structural Analysis of TORKi

The mTOR catalytic site is formed by three key regions: (i) the hinge region (Val2240); (ii) the affinity pocket (Lys2187, Glu2190, Asp2195, Try2225, Asp2357) and (iii) the solvent exposed area (Figure 2a). A N-lobe pocket delimited by Ile2163, Pro2169 and Leu2185 (purple in Figure 2a) was also classified as an important region of the ATP-binding pocket of mTOR kinase, and it is involved in inhibitor-protein interactions for a limited number of ligands (see compounds 51–54 and 58–59; Figure 7 below). The first molecules targeting the catalytic pockets of PI3Ks and both mTOR complexes were wortmannin,[18] and LY294002.[19] Following these two available pharmacological tools, the synthetic molecule PI-103 (1) was discovered.[20] PI-103 is a TORK/PI3K dual inhibitor synthesized following a high-throughput screening (HTS) aimed at identifying PI3K inhibitors.[21] The ATP-competitive inhibitor PI-103 (1) was
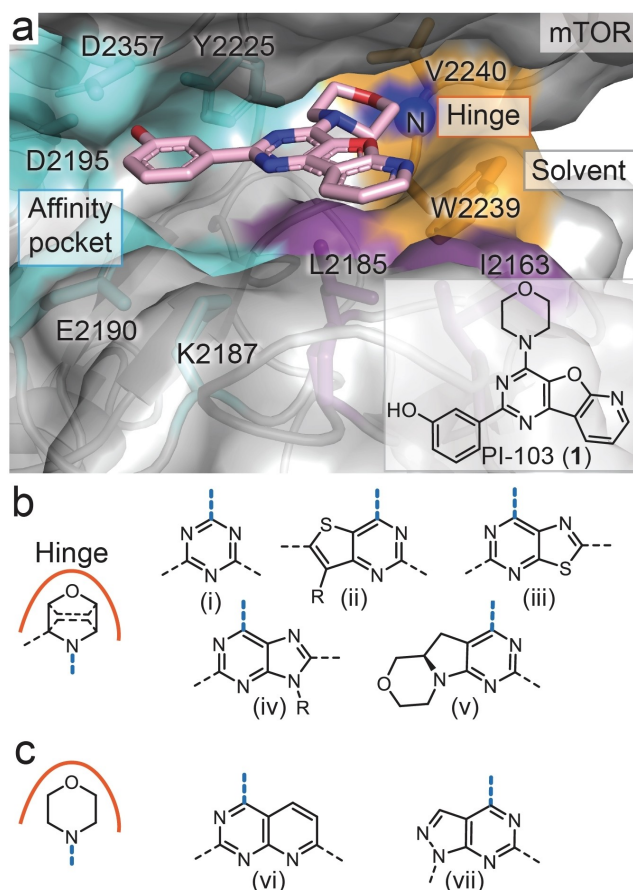
demonstrated to uniquely and potently inhibit both complexes of mTOR.[22] The co-crystal structure of mTOR kinase in complex with PI-103 (1)[1b] guided the structure-based drug design for different compound classes and helped to rationalize the binding mode of morpholine-containing TORKi.

2.1. Morpholine as Hinge Region Binder

The binding affinity pocket has been recognized as a key region in determining selectivity profiles in protein and lipid kinases.[23] Recently, also the hinge region binding has been pinpointed to play an important role in selectivity for mTOR kinase over lipid kinases. Computational studies pointed out that a leucine-phenylalanine (Leu2354 mTOR vs. Phe961 PI3Kγ) replacement leads to a deeper pocket in mTOR compared to PI3Ks.[24] Bridged morpholines are well accommodated in mTOR, but cause steric clashes in PI3K. These unfavorable steric contacts can only be minimized moving the morpholine moiety away from Val882/Val851 (in PI3Kγ/PI3Kα) impairing the pivotal H-bond to the PI3K hinge region. For a variety of chemical scaffolds, mTOR selectivity could be reached merely by the introduction of sterically hindered or methyl-substituted morpholines targeted to the hinge region of mTOR kinase. These scaffolds include (i) triazines,[25] (ii) thieno[3,2-d]pyrimidines,[26] (iii) thiazolo[5,4-d]pyrimidines,[27] (iv) purine,[27] and (v) tricyclic pyrimido-pyrrolo-oxazines[28] (Figure 2b). Bicyclic aromatic molecules such as (vi) pyrido[2,3-d]pyrimidines[29] and (vii) pyrazolo[3,4-d]pyrimidines[24,30] achieved high mTOR selectivity also with an unsubstituted morpholine interacting with the hinge Valine backbone amide (Figure 2c). In the latter case (vi and vii), the selectivity is only driven by the core and the chemical features interacting with the binding affinity region. Examples for each chemical class are described in the following sections.

2.1.1. Hinge Region Substituents as Selectivity Drivers

The morpholino- pyrimidine and triazine scaffolds have been widely investigated to modulate the PI3K/Akt/mTOR signaling pathway.[31] Dimorpholine-substituted triazines, PQR309 (Bimiralisib, 2),[32] compound 3[33] and PQR514 (4),[33] are pan-PI3K inhibitors with moderate to good mTOR affinity (Figure 3a and 3c). Starting from compound 3, replacement of one unsubstituted morpholine with a (S)-methyl substituted morpholine (PQR530, 5)[34] or an ethylene bridged-morpholine (6)[25b] did not increase mTOR selectivity. The unsubstituted morpholine of 5 and 6 is accommodated in the pocket pointing towards the hinge region Valine of mTOR and PI3K, while the sterically hindered morpholine is binding in the solvent exposed region. Introduction of two bulky morpholines on the triazine scaffold generated a highly potent and selective TORKi (PQR620, 7; Figure 3a and 3c). Compound 7 displayed a >1000-fold selectivity towards mTOR over PI3Kα in binding assays.[25b] An extensive investigation of the morpholine moiety engaging the solvent exposed region of mTOR enabled to discover PQR626 (8, Figure 3a)[25a] which maintained a good mTOR selectivity and

Figure 2. a) Key regions of the mTOR catalytic site illustrated with the PI-103-bound mTORΔN-mLST8 complex (from PDB ID: 4JT6).[1b] b, c) Selective mTOR morpholine-substituted scaffolds showing (b) a sterically hindered/substituted morpholine or (c) an unsubstituted morpholine pointing toward the hinge region Val2240. The morpholine positioning on each scaffold is reported as a blue dotted line.

ChemMedChem

Minireviews
doi.org/10.1002/cmdc.202100332

Chemistry Europe
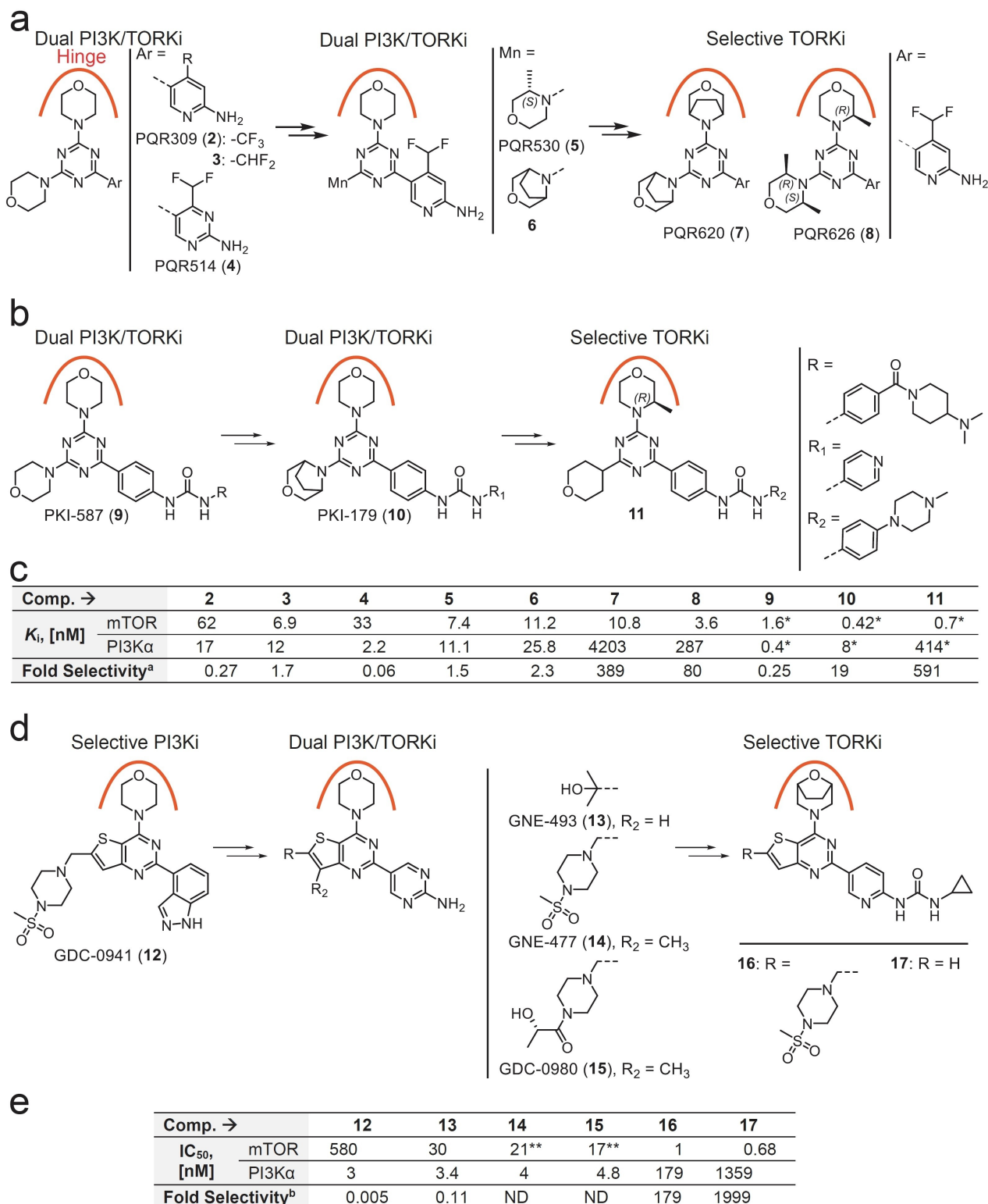European Chemical
Societies Publishing

Figure 3. Chemical investigations to develop mTOR-selective inhibitors. a) Dimorpholine-substituted triazines. b) Bis(morpholinotriazine) compounds bearing bisarylureas. c, e) Compounds potency for mTOR and PI3Kα [reported as K_i (for c) or IC_{50} (for e)] and selectivity for mTOR over PI3Kα. [a] K_i(PI3Kα)/K_i(mTOR). [b] IC_{50}(PI3Kα)/IC_{50}(mTOR). *For compounds **9**, **10** and **11** IC_{50} towards mTOR is reported instead of K_i. d) The thieno[3,2-d]pyrimidine derivatives. **14** and **15** K_i towards mTOR is reported instead of IC_{50}.

Table c:

Comp. →		2	3	4	5	6	7	8	9	10	11
K_i, [nM]	mTOR	62	6.9	33	7.4	11.2	10.8	3.6	1.6*	0.42*	0.7*
	PI3Kα	17	12	2.2	11.1	25.8	4203	287	0.4*	8*	414*
Fold Selectivity[a]		0.27	1.7	0.06	1.5	2.3	389	80	0.25	19	591

Table e:

Comp. →		12	13	14	15	16	17
IC_{50}, [nM]	mTOR	580	30	21**	17**	1	0.68
	PI3Kα	3	3.4	4	4.8	179	1359
Fold Selectivity[b]		0.005	0.11	ND	ND	179	1999

ChemMedChem

Minireviews
doi.org/10.1002/cmdc.202100332

Chemistry
Europe
European Chemical
Societies Publishing

overcome the metabolic liabilities related to the ethylene bridged morpholines. Bis(morpholinotriazine) compounds bearing bisarylureas have been also reported as potent dual PI3K/mTOR inhibitors. PKI-587 (PF-05212384, Gedatolisib, **9**)[35] is the clinically most advanced compound from this chemical class [ongoing clinical trials: NCT03698383, NCT03911973, NCT03065062, NCT02626507]. As expected, installation of only one sterically demanding 3,5-ethylene bridged morpholine on the triazine core (PKI-179, **10**) did not lead to mTOR-selective inhibition (Figure 3b).[36] The combination of a (R)-methyl substituted morpholine and a tetrahydropyran (THP, compound **11**) resulted in a potent and selective mTOR inhibitor [selectivity $IC_{50}(PI3K\alpha)/IC_{50}(mTOR) = 591$, Figure 3c].[25c] The THP of compound **11** binds in the solvent exposed region, while the substituted morpholine is accommodated into the hinge pocket of mTOR. The ability of the THP and 3,6-dihydro-2H-pyran (DHP) to function as morpholine surrogates has been explored on different scaffolds [thienopyrimidine (ii) and pyrazolopyrimidine (vii)]. Only DHP has been pinpointed as a morpholine bioisostere. Computational studies revealed that DHP and morpholine moieties establish the same essential H-bond to Val2240 in mTOR, while the out of plane conformation of the THP residue cannot interact with the backbone amide of the hinge region Valine.[37] The thieno[3,2-d]pyrimidine scaffold has been extensively explored for the development of dual PI3K/mTOR inhibitors. Starting from GDC-0941 (Pictilisib, **12**),[38] a class I PI3K inhibitor, chemical modifications were introduced to increase potency for mTOR and develop dual PI3K/mTOR inhibitors. GNE-493 (**13**),[39] GNE-477 (**14**),[40] and GDC-0980 (Apitolisib, **15**)[41] have been developed as inhibitors targeting both class I PI3Ks and mTOR kinase (Figure 3d). Installation of an 8-oxa-3-azabicyclo[3.2.1]octane group onto a thienopyrimidine scaffold significantly increased the selectivity for mTOR over PI3Kα (compounds **16** and **17**, Figure 3d and 3e), with compound **17** displaying a >1000-fold potency for mTOR over the structurally related class I PI3Ks.[26] The 4-ureidophenyl group played also a key role in driving selectivity (see 2.2). Chemical investigation of the thienopyrimidine scaffold led to the design of compounds bearing the related purine scaffold. The tricyclic molecule containing the purine core, Paxalisib (GDC-0084, **18**; Figure 4a and 4d), is a dual inhibitor of PI3K and mTOR kinases, showing a desirable pharmacokinetic profile.[42] However, substituted and sterically hindered morpholines have not been appended on the tricyclic purine-based scaffold and no selective mTOR inhibitors have been developed from this scaffold. The purine core is also present in a dual PI3K/mTOR inhibitor, DS-7423 (**19**),[43] and in a selective mTOR molecule (**20**, Figure 4b and 4d). While DS-7423 presents an unsubstituted morpholine, compound **20** has a (R)-3-methylmorpholine pointing towards the hinge Valine. The (R)-3-methylmorpholine has been described as an optimal moiety to establish a H-bond with the backbone of Val2240 in mTOR and to provide selectivity over the closely related PI3K family.[27] This substituted morpholine has been exploited as mTOR selector in different chemotypes, including triazines (**8**, **11**, Figure 3b), thiazolo[5,4-d]pyrimidine and tricyclic pyrimido-pyrrolo-oxazines. The purine core of **20** was converted into a thiazolo[5,4-d]
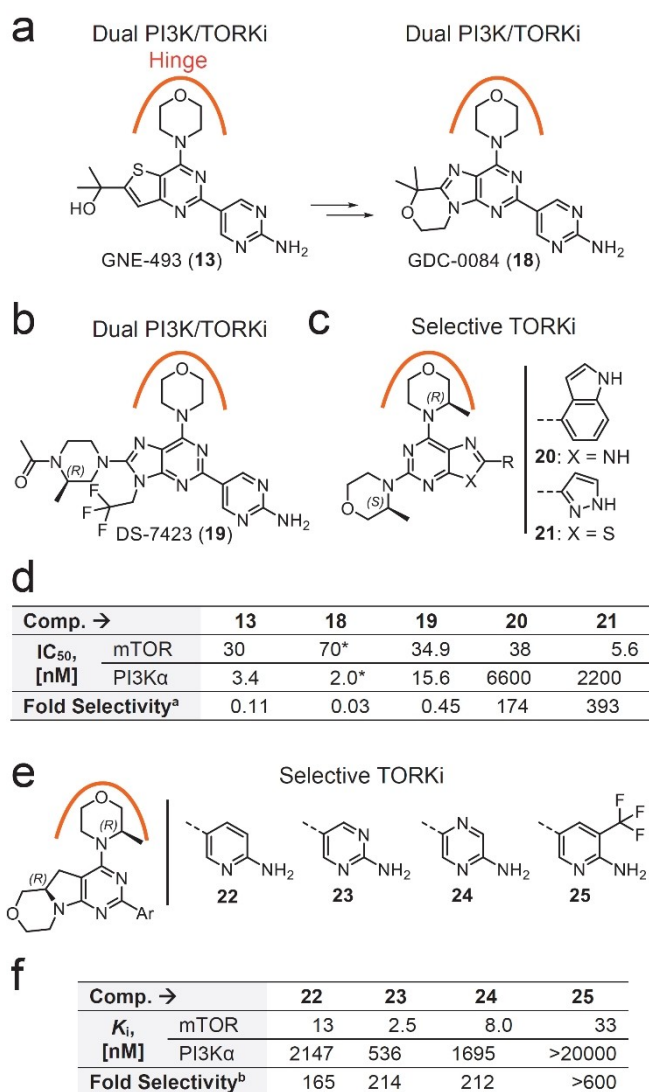

Figure 4. Chemical development of a tricyclic molecule containing the purine core, purines, thiazolo[5,4-d]pyrimidines, and tricyclic pyrimido-pyrrolo-oxazine derivatives. a, b) An unsubstituted hinge region morpholine prevented the development of highly selective purine-based mTOR inhibitors. c, e) (R)-3-methylmorpholine enabled the development of purine-, thiazolo[5,4-d]pyrimidine-based and tricyclic pyrimido-pyrrolo-oxazine mTOR-selective binders. The hinge region is schematically reported (orange). d, f) Compounds potency for mTOR and PI3Kα [reported as IC_{50} (for d) or as K_i (for f)] and selectivity for mTOR over PI3Kα. [a] $IC_{50}(PI3K\alpha)/IC_{50}(mTOR)$. * K_i values are reported for compound **18**. [b] $K_i(PI3K\alpha)/K_i(mTOR)$.

pyrimidine and the physicochemical space investigated. Compound **21** showed an improved potency as compared to **20**, and optimized physicochemical properties.[27] For the (R)-configured tricyclic pyrimido-pyrrolo-oxazine scaffold, a (S)-3-methylmorpholine slightly increased the potency and selectivity for mTOR as opposed to unsubstituted hinge region morpholines.[28a] The (R)-3-methylmorpholine yielded the best mTOR selectivity of this series of conformationally restricted molecules. Extensive SAR studies allowed to pinpoint compounds **22–25** as highly selective mTOR inhibitors with a variety of profiles regarding brain penetration and physicochemical properties.[28] Among them, **25**[28b] displayed the highest

ChemMedChem

Minireviews
doi.org/10.1002/cmdc.202100332

Chemistry Europe
European Chemical
Societies Publishing

selectivity [K_i(PI3Kα)/K_i(mTOR) > 600; Figure 4e and 4f]. For the compounds' classes described in this sub-chapter, substituted and sterically hindered morpholines are pivotal to direct mTOR selectivity, but alone they are not able to yield highly selective inhibitors.

To selectively bind mTOR kinase, a combination of (i) modified hinge region-binding morpholines and (ii) properly substituted heteroaromatic moieties accommodating in the binding affinity pocket is required.

2.2. Core and Binding Affinity Region Moieties as Selectivity Drivers

Bicyclic aromatic pyrimidines achieve high mTOR selectivity with unsubstituted morpholines pointing towards the hinge region valine. A high throughput screen carried out by a collaboration between KuDOS Pharmaceuticals and AstraZeneca identified the pyrido[2,3-d]pyrimidine-2,4-diamine as a promising scaffold for the development of small molecule mTOR inhibitors. Variations of the core highlighted that position 8 of the bicyclic core is the optimal placing for the pyridine nitrogen. The solvent exposed morpholine has been explored and sub-micromolar mTOR inhibitors have been identified (compounds **26** and **27**; Figure 5a and Figure 5c). The introduction of aromatic substituents in position 7 of the core scaffold resulted in enhancement of potency, with an excellent selectivity of KU0063794 for mTOR over PI3Ks [**28**, IC$_{50}$(PI3Kα)/IC$_{50}$(mTOR) = 556; Figure 5a].[44] An H-bond donor on the aromatic moiety was postulated to be essential for the binding. Further investigation of this compound series was required to deliver clinical candidates since **28** displayed low aqueous solubility, and human ether-a-go-go related gene (hERG) liability. In drug discovery programs, early identification of potential hERG inhibition allows to reduce the risk of drug candidates failing in preclinical and clinical trials.[45] Introduction of a (S)-3-methyl morpholine enhanced cellular potency leading to AZD8055 (**29**) which displayed excellent selectivity for mTOR kinase over PI3K (Figure 5a).[46] The benzyl alcohol and the aryl-methyl ether of **28** and **29** were identified as potential metabolic liabilities. Thus, different chemical modifications on the aromatic ring were carried out to reduce the turnover in human hepatocytes and yielded AZD2014 (Vistusertib, **30**; Figure 5a and 5c) overcoming the drawbacks of the previous pyrido[2,3-d]pyrimidine derivatives. Compound **30** displayed excellent mTOR affinity and selectivity, negligible interference with hERG, excellent aqueous solubility and good oral expose.[29] Beside compound **28**, additional highly selective mTOR inhibitors showing an unsubstituted morpholine interacting with the backbone amide of Val2240 have been reported. These molecules contain a pyrazolopyrimidine core and were discovered in a lead optimization process starting with WAY-001 (**31**, Figure 5b), which was identified thought an HTS campaign. The starting hit **31** was 6-fold more potent towards PI3Kα than mTOR.[47] Hit expansion produced pyrazolopyrimidine **32**, a dual PI3K/TORKi (Figure 5b). However, the metabolic liabilities of the phenolic group prompted SAR studies to

increase potency, selectivity and metabolic stability of pyrazolopyrimidines. Replacement of the phenol with an indole ring led to the identification of WAY-600 (**33**) displaying a good mTOR selectivity [IC$_{50}$(PI3Kα)/IC$_{50}$(mTOR) = 218, Figure 5b and Figure 5c].[30a] Subsequent chemical exploration on the moiety engaging the mTOR binding affinity region and on the piperidine pointing towards the solvent exposed pocket led to the identification of WYE-354 (**34**), **35** and **36**, showing excellent mTOR selectivities [IC$_{50}$(PI3Kα)/IC$_{50}$(mTOR) = 239, 681 and 1153, respectively; Figure 5b and 5c]. Both carbamate and urea have been identified as pivotal moieties for binding into the mTOR affinity pocket due to the establishment of H-bonds (i) between the carbamate/urea NH(s) and Asp2195, and (ii) the carbonyl and Lys2187.[48] Extensive studies on the ureidophenyl substituents highlighted their ability to control the selectivity versus PI3Ks.[30b] As previously discussed, bridged morpholines are well accommodated into mTOR hinge region but lead to steric clashes in PI3K (see 2.1). A 2,6-bridged morpholine has been appended on the pyrazolopyrimidine scaffold. Compounds **37**, **38** and WYE-132 (WYE-125132, **39**), bearing the same substituted morpholine and urea-containing aromatic ring, showed sub-nanomolar mTOR IC$_{50}$s together with remarkable selectivity (Figure 5d and 5f).[24,49] The presence of a bridged morpholine boosted selectivity of pyrazolopyrimidine derivatives independently from the substituents on the pyrazole ring. Also compound **38** displaying a trifluoroethyl moiety is a potent, and specific inhibitor of mTOR kinase. Piperazinophenyl urea derivatives **40** and **41** maintained an acceptable mTOR selectivity due to the presence of the 2,6-bridged morpholine [IC$_{50}$(PI3Kα)/IC$_{50}$(mTOR) = 250 and 170, respectively, Figure 5d and 5f]. In addition, the piperazine moiety increased both cellular activity and human microsomal stability compared to the unsubstituted phenyl analogs.[50] Replacement of the pyrazole with a triazole moiety, and introduction of the urea substitution present in PKI-587 (**9**, Figure 3b) resulted in the discovery of PKI-402 (**42**, Figure 5e) showing low nanomolar potency against both PI3Kα and mTOR (Figure 5f).[51]

2.3. Hinge Region Binders Different from Morpholines

Molecules showing a variety of chemical moieties responsible for the H-bond with the hinge region Valine were discovered. The pyrazolopyrimidine scaffold was proposed as adenine-mimetic and exploited in tyrosine kinase,[52] PI3K and mTOR inhibitors. A library of tyrosine kinase inhibitors was screened for activity against PI3Kα and, after hits identification, an extensive SAR study was carried out to identify the chemical features favoring the interactions with PI3K. PP242 (Torkinib, **43**) displayed an unexpected selectivity for mTOR, being the first described selective and ATP-competitive mTOR inhibitor (Figure 6a and 6e).[53] X-ray crystallographic structure of mTOR kinase in complex with **43** shed light on the unpredicted profile: Yang et al. revealed that upon **43** binding, mTOR underwent a conformational change involving the side chains of Tyr2225, Gln2223 and Leu2354. This resulted in an expansion and deepening of the inner hydrophobic pocket accommodating
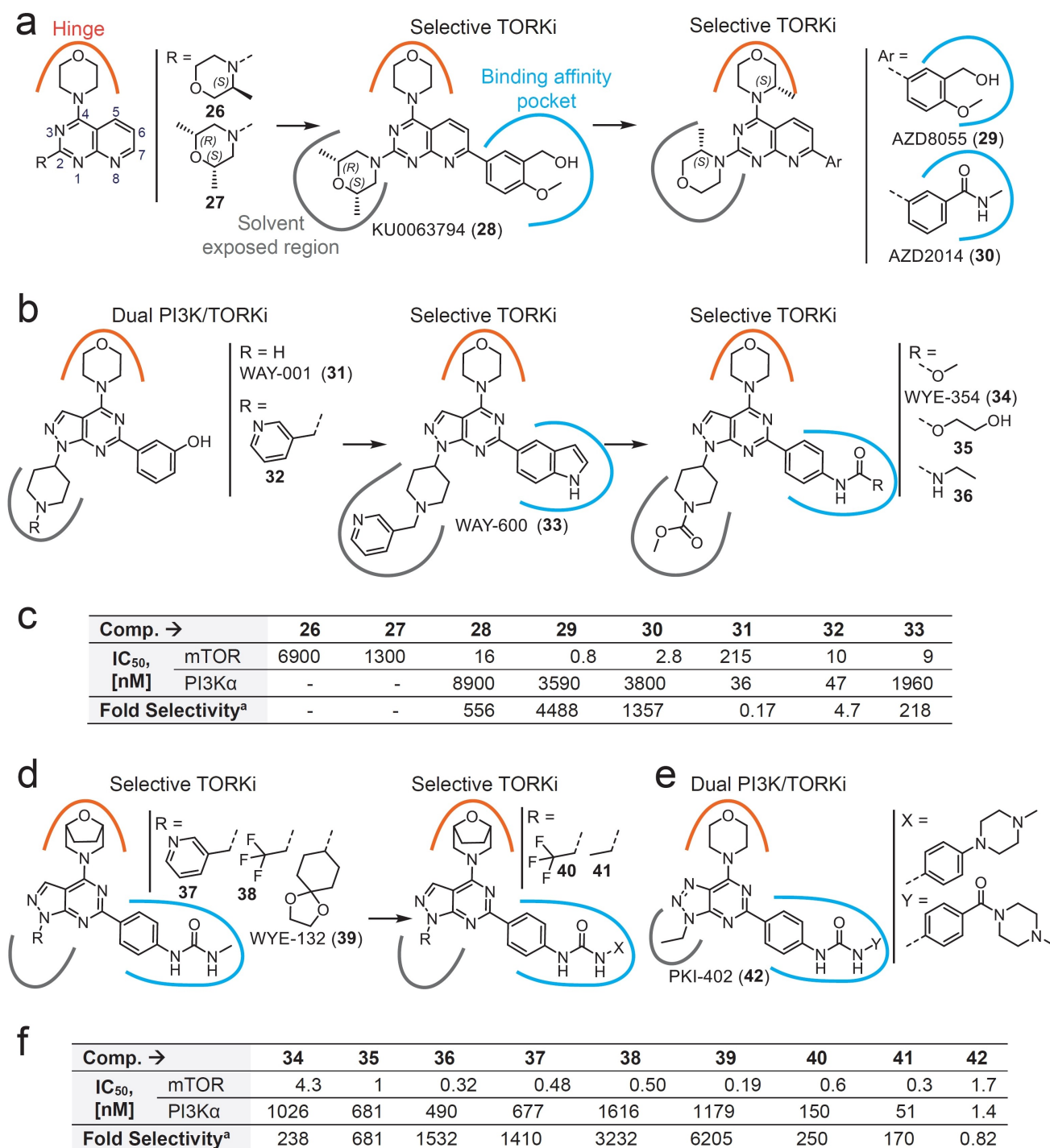
ChemMedCrem

Minireviews
doi.org/10.1002/cmdc.202100332

Chemistry
Europe
European Chemical
Societies Publishing

Figure 5. SAR studies on (a) pyrido[2,3-d]pyrimidine-2,4-diamines and (b, d) pyrazolopyrimidine for the identification of highly selective mTOR inhibitors. The compounds binding mode into mTOR is schematically reported (orange, hinge region; cyan, binding affinity pocket; gray, solvent exposed region). e) Urea-substituted 7-morpholinotriazolopyrimidine, PK-402 (42), as dual PI3K/mTOR inhibitor. c, f) Compounds' potency for mTOR and PI3Kα (reported as IC$_{50}$) and selectivity for mTOR over PI3Kα. [a]IC$_{50}$(PI3Kα)/IC$_{50}$(mTOR).

the hydroxyindole moiety (Figure 6b and 6c).[1b] In the hinge region, the 4-aminopyrazolo[3,4-d] pyrimidine core forms two hydrogen bonds with the backbone amide nitrogen of Val2240 and the backbone oxygen of Gly2238. Starting from 43, a structure-guided optimization led to the identification of a pyrazolopyrimidine derivative (INK128, 44; Figure 6a and 6e)

with improved oral bioavailability and pharmaceutical properties suitable for clinical studies.[54] At the same time, Celgene carried out a HTS which identified an imidazo[4,5-b]pyrazin-2-one (45) as hit showing micromolar potency towards mTOR (Figure 6d). A broad hit-to-lead optimization led to the identification of CC214 (46), 47 and 48 with excellent mTOR potency
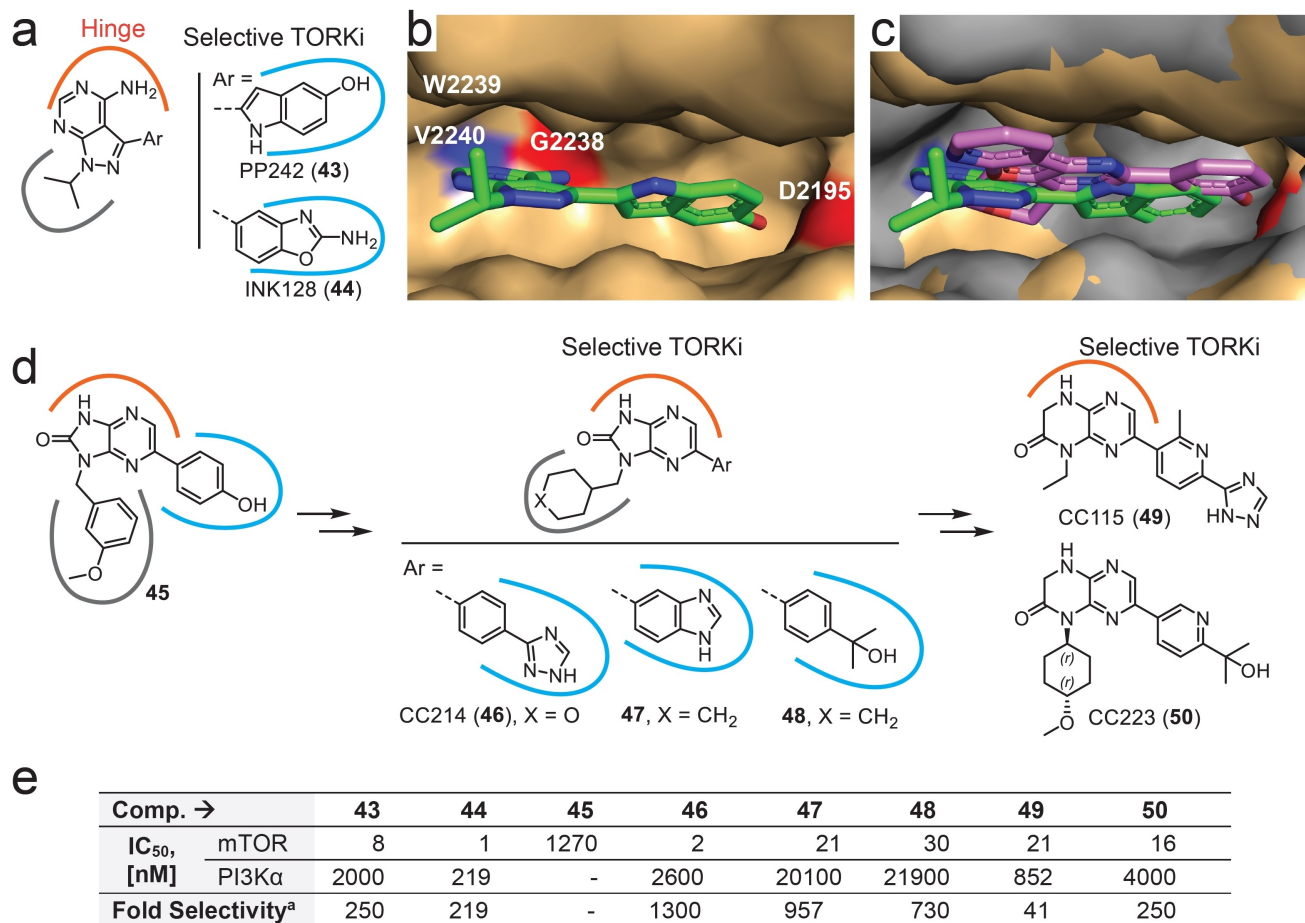
ChemMedChem

Minireviews
doi.org/10.1002/cmdc.202100332

Chemistry
Europe
European Chemical
Societies Publishing

Figure 6. 4-Aminopyrazolo[3,4-*d*] pyrimidines and dihydropyrazino[2,3-b]pyrazin-2(1*H*)-ones as hinge region binding modules. a) Chemical structures of PP242 (**43**) and INK128 (**44**). b) X-ray crystallographic structure of mTOR kinase (sand, surface) in complex with PP242 (green, PDB ID 4JT5). c) Comparison between mTOR-PP242 and mTOR-PI-103 (mTOR, gray surface; PI-103, pink; PDB ID 4JT6)[1b] complexes revealed a deeper inner hydrophobic pocket induced upon PP242 binding. d) Hit identification and hit-to-lead optimization leading to the discovery of CC115 (**49**) and CC223 (**50**). The compounds binding mode into mTOR is schematically reported (orange, hinge region; cyan, binding affinity pocket; gray, solvent exposed region). e) Compounds potency for mTOR and PI3Kα (reported as IC$_{50}$) and selectivity for mTOR over PI3Kα. [a]IC$_{50}$(PI3Kα)/IC$_{50}$(mTOR). CC115 inhibits in a low nanomolar concentration also DNA-PK (IC$_{50}$=13 nM).

and exquisite kinase selectivity [IC$_{50}$(PI3Kα)/IC$_{50}$(mTOR) > 730; Figure 6d and 6e].[55] Scaffold hopping starting from the imidazo [4,5-*b*]pyrazin-2-one derivatives enabled to discover a new series of mTOR binders displaying the dihydropyrazino[2,3-*b*] pyrazin-2(1*H*)-one core. Parallel SAR explorations pinpointed CC115 (**49**)[56] and CC223 (Onatasertib, **50**)[57] as clinical candidates (Figure 6d). While **50** selectively targets mTOR kinase (Figure 6e), **49** is a dual inhibitor of mTOR (IC$_{50}$=21 nM) and DNA-dependent protein kinase (DNA-PK, IC$_{50}$=13 nM). A medium throughput cell-based screening assay followed by structure-guided drug design was employed also for the identification of Torin 1 (**53**)[58] and Torin 2 (**54**).[59] A combinatorial kinase-directed library[60] screening led to the identification of the quinoline hit compound **51** exhibiting moderately in vitro inhibitory activity. The introduction of an additional ring constraint resulted in a benzonaphthyridinone compound **52**, which exhibited a 1000-fold improved mTOR affinity as compared to **51** (Figure 7a and 7e). Chemical design guided by cell-based SAR studies combined with molecular modeling

enabled the development of **53** with 900-fold selectivity for mTOR over PI3K.[58a,61] **53** is a good chemical probe, but its short half-life, poor water solubility, and limited bioavailability prompted a lead optimization process. Compound **54** emerged from an extensive medicinal chemistry campaign aimed at the optimization of the pharmacokinetic profile and synthetic accessibility (Figure 7a and 7e).[59] The X-ray crystallographic structure of mTOR$^{\Delta N}$– mLST8 bound to **54** (PDB ID 4JSX) was solved, and the benzonaphthyridinone moiety was found to be involved in the H-bond with the backbone amide of Val2240 (Figure 7b). The tricyclic core is responsible for an extensive stacking interaction with the indole ring of Trp2239 in the hinge region. The tryptophan-valine replacement (Trp2239, mTOR; Val850, PI3Kα) is likely to contribute to the 800-fold specificity of **54** for mTOR over PI3Kα. The aminopyridine group of **54** is accommodated into the binding affinity pocket. Interestingly the amino group is not involved in H-bonds with Asp2195, Asp2357 and Try2225, residues that have been defined as key interactions in PP242 (**43**, PDB ID 4JT5; Figure 7c) and PI-103 (**1**,
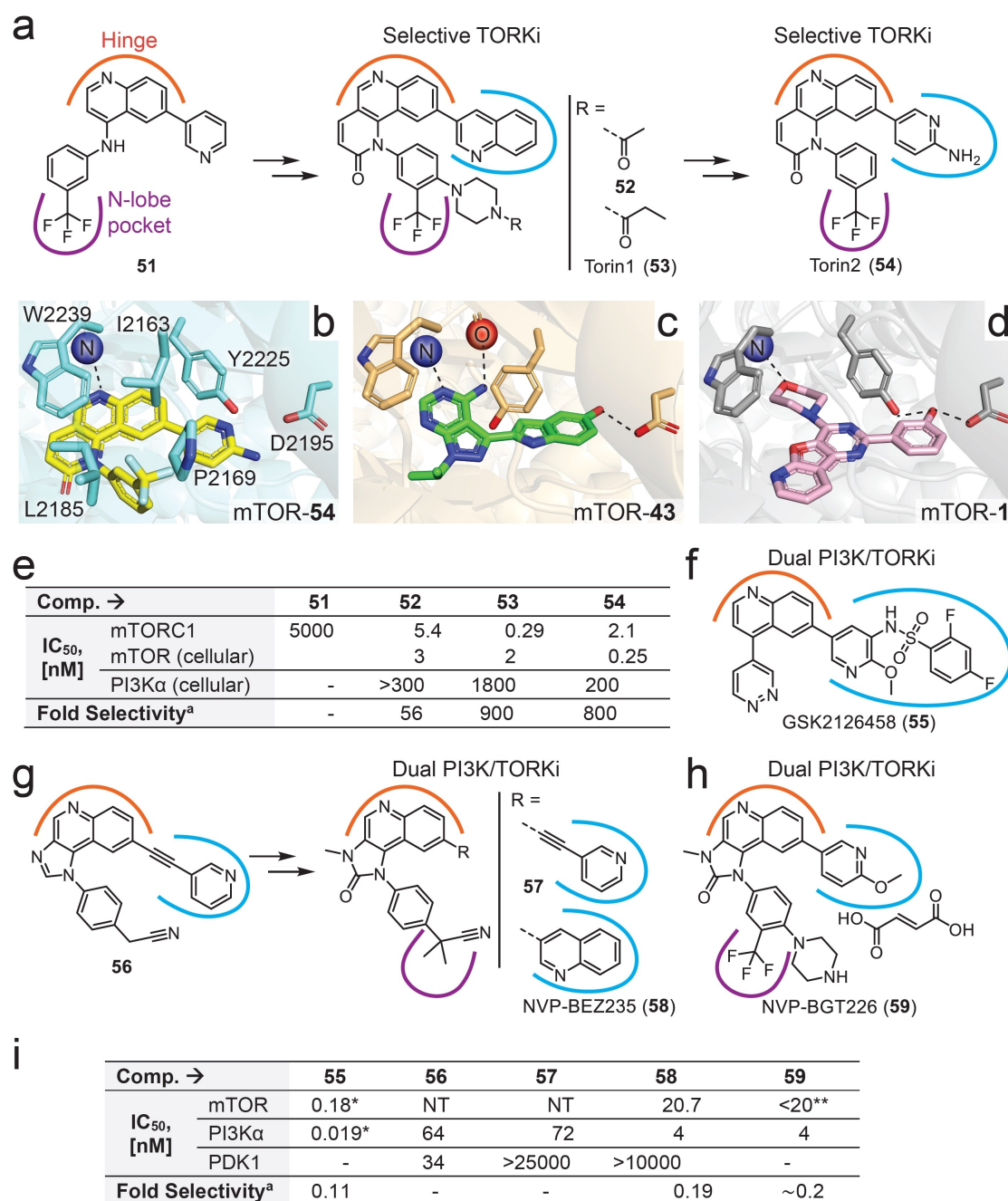
ChemMedChem

Minireviews
doi.org/10.1002/cmdc.202100332

Chemistry Europe
European Chemical
Societies Publishing

Figure 7. Analysis of chemical structure, binding mode and biological activity of quinonoline derivatives. a) Identification of the benzonaphthridinone derivatives, Torin1 (**53**) and Torin2 (**54**). The compounds binding mode to mTOR is schematically reported (orange, hinge region; cyan, binding affinity pocket; purple, N-lobe pocket). b, c, d) Comparison of 3 X-ray crystallographic structures: mTOR (cyan) – **54** (yellow; b, PDB ID: 4JSX); mTOR (sand) – **43** (green, c, PDB ID: 4JT5); mTOR (gray) – **1** (pink; d, PDB ID: 4JT6)[1b] The NH backbone amide of V2240 is shown as blue sphere (in b, c, d). The carbonyl O of Gly2238 backbone amide is represented as red sphere (in c). H-bonds are displayed as black dotted lines. e, i) Compounds potency for mTOR and PI3Kα (reported as IC$_{50}$) and selectivity for mTOR over PI3Kα. [a] IC$_{50}$(PI3Kα)/IC$_{50}$(mTOR). * K_i values. ** Approximate value as reported in Ref. [62]. f, g, h) Chemical structure of dual PI3K/mTOR inhibitors bearing a quinoline or a imidazo[4,5-c]quinoline core.

PDB ID 4JT6; Figure 7d) binding.[1b] The quinoline is considered a privileged scaffold for ATP-site binders and it is present, alone or fused to other rings, in several mTOR inhibitors. The quinoline core is the building block of Omipalisib (GSK2126458, GSK458, **55**), which shows picomolar affinity for PI3Kα and mTOR (Figure 7f and 7i). In addition, **55** is a potent inhibitor of DNA-PK (IC$_{50}$ = 0.28 nM), a member of the PIKK family.[63] Beside

quinoline, the imidazo[4,5-c]quinoline scaffold can mimic the H-bond interactions of the ATP adenine moiety and has been exploited in different drug discovery programs aiming at the identification of PI3K and mTOR inhibitors. This chemotype is present in NVP-BEZ235 (Dactolisib, **58**, Figure 7g),[64] a dual PI3K/mTOR inhibitor showing anti-tumor efficacy in mouse models[65] and investigated in several Phase I and II clinical trials.

These are not the final page numbers! ⌐⌐

ChemMedChem

Minireviews
doi.org/10.1002/cmdc.202100332

Chemistry
Europe
European Chemical
Societies Publishing

58 was developed starting from a 3-phosphoinositide-dependent protein kinase 1 (PDK1) inhibitor (**56**) able to inhibit also class I PI3K.[66] The introduction of a *N*-methyl imidazol-2-one moiety (compound **57**) resulted in a complete loss in PDK1 inhibitory activity, while the PI3K affinity was retained (Figure 7g and 7i). Afterwards, a quinoline was appended on the 3-methylimidazo[4,5-*c*]quinolin-2-one core leading to the development of compound **58** (Figure 7g).[64,67] Medicinal chemistry efforts merging compounds **53** and **58** resulted in the discovery of the dual PI3K/mTOR inhibitor NVP-BGT226 (**59**, Figure 7h).[62] Compounds **58** and **59** are extremely lipophilic molecules with clogP > 5 (see 3.2).

3. Effect of Physicochemical Descriptors on Brain Permeability

3.1. Accessing the Brain: A Major Drug Discovery Challenge

Although there are > 60 FDA-approved kinase inhibitors,[68] none of them has been approved for the treatment of primary CNS tumors or neurodegenerative disease.[69] Alectinib received accelerated approval for anaplastic lymphoma kinase (ALK) positive metastatic non-small cell lung cancer (NSCLC) to treat patients including those with brain metastases.[70] Entrectinib is another tyrosine kinase inhibitor (TKI) targeting ALK and ROS1 (ROS Proto-Oncogene 1, Receptor Tyrosine Kinase), which penetrates the BBB and has shown efficacy in ROS1-positive NSCLC brain metastases.[71] Tucatinib is quinazoline-triazolo[1,5-*a*]pyridine derivative approved to treat patients with HER2-positive metastatic breast cancer with brain metastases.[72] In 2018, everolimus (Afinitor), an allosteric inhibitor of TORC1, was approved by FDA for the treatment of tuberous sclerosis complex (TSC) associated seizures.[73]

Developing molecules able to access the CNS and to reach an optimal concentration at the therapeutic target is a challenging endeavor in drug discovery.[74] The central role of mTOR signaling in neurological disease fueled the interest in molecules able to cross the BBB. Physicochemical properties required for brain access have been extensively investigated,[75] and a rule of 5 (Ro5)[76] has been proposed for CNS drugs.

3.2. Physicochemical Properties of TORKi

Lipophilicity is considered the most important drug-like physical property affecting potency, distribution and elimination of a drug.[77] Increasing lipophilicity often correlates with improved binding affinities; however, it also increases non-specific binding to multiple targets resulting in toxic effects.[78] The LogP [Log of the octanol-water partition coefficient] is the measure of drugs lipophilicity. High lipophilicity is accompanied by poor aqueous solubility and high metabolic turnover. Lipophilicity also affects CNS exposure,[79] and kinase inhibitors were classified as having higher lipophilicity compared to approved CNS drugs. While a median clogP value of 4.2 has been

reported for approved kinase inhibitors, the drugs currently used to treat CNS disorders have a median clogP of 2.8.[69,80] Hansch et al. proposed that the optimal CNS penetration occurs with compounds possessing logP ~ 2, with an acceptable range between 2 and 5.[81]

We calculated a mean clogP of 3.2 for inhibitors **1**–**59** (Figure 8a), which is higher than approved CNS drugs. Most of the described mTOR inhibitors displayed clogP values between 2 and 4, with outliers being CC115 (**49**) and NVP-BEZ235 (**58**), showing clogP of −0.5 and 6.3, respectively (Figure 8d). Compound **49** is in phase II clinical trials for the treatment of glioblastoma [NCT02977780], but neither brain:plasma ratio (B/P) or efflux properties have been published. Brain penetration of **58** is counteracted by Abcb1, a drug efflux transporter expressed in the BBB, which limits CNS target engagement.[82] Beside lipophilicity, physicochemical properties like molecular weight (MW), polar surface area (PSA), and the number of hydrogen-bond donors (HBD) and acceptors (HBA) influence brain penetration.[83] MW, which can be calculated with accuracy, is considered a descriptor to predict other properties: often an increase in MW results in an increased lipophilicity.[84] This general trend is also observed with mTOR inhibitors (Figure 9a). CNS drugs are in general smaller than non-BBB penetrating drugs. Van de Waterbeemd and others defined a MW < 450 Da as desirable for CNS drug candidates,[83c,85] and the median MW for marketed CNS drugs has been reported to be ~ 305.[75b,c] The inhibitors described here have a mean MW of ~ 426 Da (Figure 8b), spanning MW from 315 (**26**) to 622 (**40**). Compound **26** (Figure 5a) is a hit identified through HTS showing a moderate mTOR potency due to lack of a binding module targeting the affinity region. **40** is a potent and selective mTOR inhibitor (Figure 5d and 5f) discovered through extensive medicinal chemistry campaigns. It has not been investigated regarding brain penetration (Figure 8d). The polar surface area (PSA) is a physicochemical descriptor which plays a key role in the design of compounds with potential BBB penetration. P-glycoprotein (P-gp, multi-drug resistance protein MDR1, ABCB1) is an efflux transporter with protective function for the BBB. Chemical species identified as P-gp substrates are classified as non-CNS drugs.[86] To minimize P-gp action, Hitchcock proposed a PSA < 90 Å^2 (preferably < 70 Å^2) and a HBD count < 2. Compounds **1**–**59** showed a median PSA value of 101 Å^2 (Figure 8c), being double to that of the approved CNS drugs.[69] Compounds **12** and **14** did not penetrate the BBB, which might be due to the detrimental influence of the polar sulfone group that dramatically increases PSA (144 and 167 Å^2, respectively). Similarly, the thieno[3,2-*d*] pyrimidines **13** and **15** showed a PSA higher than 135 Å^2 leading to a lack in brain penetration.[69] The only sulphur-containing TORKi able to access the brain was the thiazolo[5,4-*d*]pyrimidine **21**, displaying a PSA of 121 Å^2.[27] Among the brain penetrant TORKi, only compound **25** showed a PSA < 90 Å^2. Interesting, although **58** had a PSA equal to 73 Å^2, it did not show a good CNS exposure due to the excessive lipophilicity (Figure 8d). The number of HBD has been also recognized as a critical property for brain permeability since it affects the P-gp mediated efflux. Hydrogen bond donors are usually present in ATP-competitive kinase
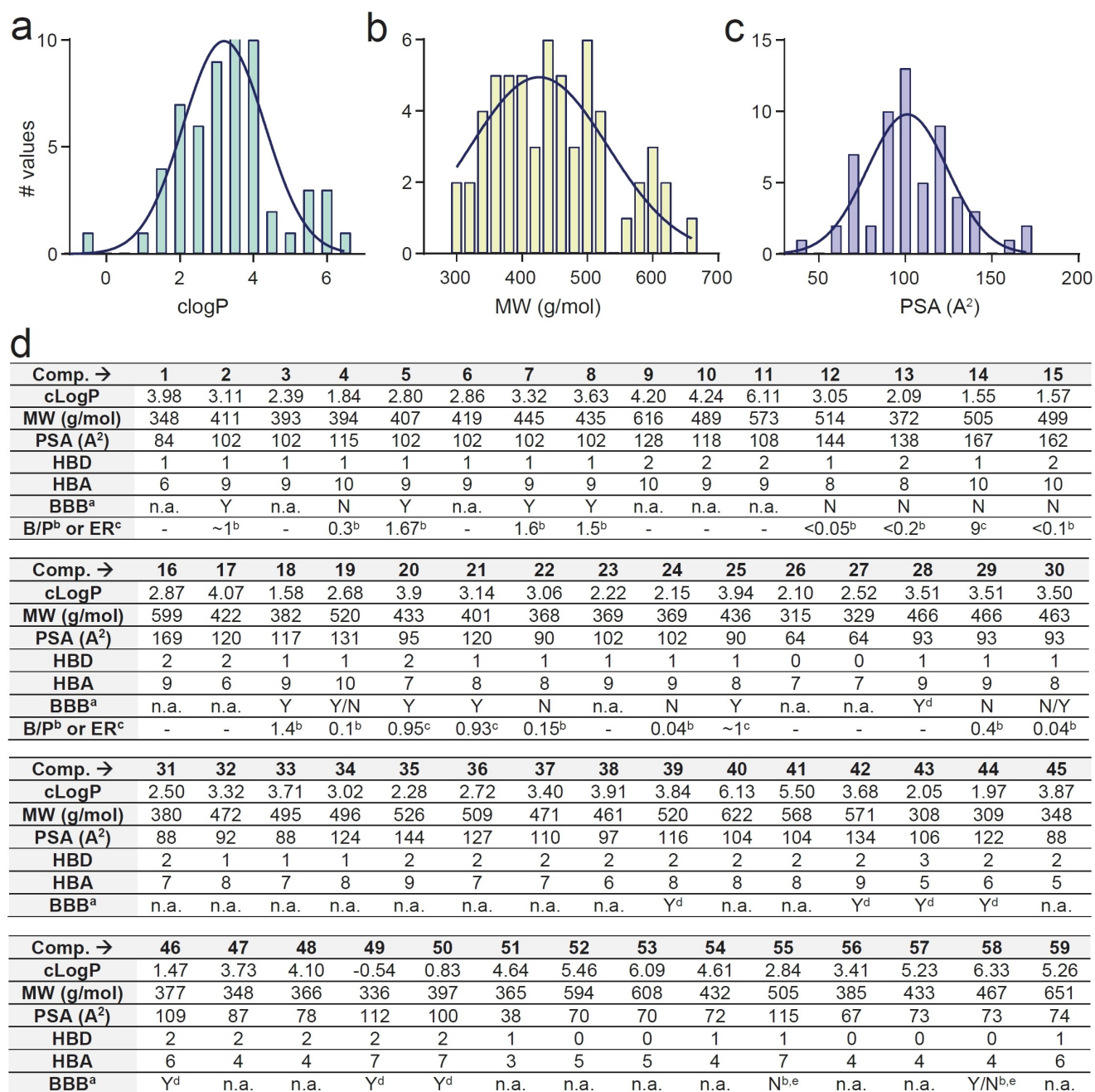
Figure 8. Physicochemical properties and BBB distribution of compounds **1–59**. a, b, c) Histogram to show frequency distribution of a) cLogP, b) MW, c) PSA. Mean value of MW = 426.2, cLogP = 3.2 and PSA = 101.1. d) Summary of physicochemical properties, BBB permeability, Brain/Plasma ratio (B/P) or Efflux Ratio (ER) of compounds **1–59**. Marvin/JChem 20.20 was used for calculation of cLogP (partition coefficient), PSA (Polar Surface Area), HBD (Hydrogen Bond Donor) and HBA (Hydrogen Bond Acceptor) values. [a] BBB permeability: BBB-permeable inhibitors (Y, Yes); non-BBB-permeable inhibitors (N, No). n.a. = not available information regarding brain penetration. [b] B/P ratio assessed through pharmacokinetic (PK) studies (in vivo). [c] ER assessed using a MDCK-MDR1 permeability *in vitro* assay. [d] Brain exposure and transporter-mediated efflux data are not available, however the compounds show efficacy in animals model for brain disease (**28, 39, 42, 43, 46**) or are investigated in clinical trials for brain tumors (**44, 49, 50**). [e] Limited (**58**) or lack of (**55**) brain permeability is related to transport-mediated efflux [substrate for Bcrp (breast cancer resistance protein) and/or P-gp]. B/P ratio: **55** = 0.06;[87] **58** = 0.7.[82] Marvin/JChem 20.9 was used to calculate logP, PSA, HBD and HBA values, ChemAxon (https://www.chemaxon.com). ChemDraw Professional 16.0 was used to calculate MW.

Comp. →	1	2	3	4	5	6	7	8	9	10	11	12	13	14	15
cLogP	3.98	3.11	2.39	1.84	2.80	2.86	3.32	3.63	4.20	4.24	6.11	3.05	2.09	1.55	1.57
MW (g/mol)	348	411	393	394	407	419	445	435	616	489	573	514	372	505	499
PSA (A²)	84	102	102	115	102	102	102	102	128	118	108	144	138	167	162
HBD	1	1	1	1	1	1	1	1	2	2	2	1	2	1	2
HBA	6	9	9	10	9	9	9	9	10	9	9	8	8	10	10
BBB[a]	n.a.	Y	n.a.	N	Y	n.a.	Y	Y	n.a.	n.a.	n.a.	N	N	N	N
B/P[b] or ER[c]	-	~1[b]	-	0.3[b]	1.67[b]	-	1.6[b]	1.5[b]	-	-	-	<0.05[b]	<0.2[b]	9[c]	<0.1[b]

Comp. →	16	17	18	19	20	21	22	23	24	25	26	27	28	29	30
cLogP	2.87	4.07	1.58	2.68	3.9	3.14	3.06	2.22	2.15	3.94	2.10	2.52	3.51	3.51	3.50
MW (g/mol)	599	422	382	520	433	401	368	369	369	436	315	329	466	466	463
PSA (A²)	169	120	117	131	95	120	90	102	102	90	64	64	93	93	93
HBD	2	2	1	1	2	1	1	1	1	1	0	0	1	1	1
HBA	9	6	9	10	7	8	8	9	9	8	7	7	9	9	8
BBB[a]	n.a.	n.a.	Y	Y/N	Y	Y	N	n.a.	N	Y	n.a.	n.a.	Y[d]	N	N/Y
B/P[b] or ER[c]	-	-	1.4[b]	0.1[b]	0.95[c]	0.93[c]	0.15[b]	-	0.04[b]	~1[c]	-	-	-	0.4[b]	0.04[b]

Comp. →	31	32	33	34	35	36	37	38	39	40	41	42	43	44	45
cLogP	2.50	3.32	3.71	3.02	2.28	2.72	3.40	3.91	3.84	6.13	5.50	3.68	2.05	1.97	3.87
MW (g/mol)	380	472	495	496	526	509	471	461	520	622	568	571	308	309	348
PSA (A²)	88	92	88	124	144	127	110	97	116	104	104	134	106	122	88
HBD	2	1	1	1	2	2	2	2	2	2	2	2	3	2	2
HBA	7	8	7	8	9	7	7	6	8	8	8	9	5	6	5
BBB[a]	n.a.	n.a.	n.a.	n.a.	n.a.	n.a.	n.a.	n.a.	Y[d]	n.a.	n.a.	Y[d]	Y[d]	Y[d]	n.a.

Comp. →	46	47	48	49	50	51	52	53	54	55	56	57	58	59
cLogP	1.47	3.73	4.10	-0.54	0.83	4.64	5.46	6.09	4.61	2.84	3.41	5.23	6.33	5.26
MW (g/mol)	377	348	366	336	397	365	594	608	432	505	385	433	467	651
PSA (A²)	109	87	78	112	100	38	70	70	72	115	67	73	73	74
HBD	2	2	2	2	2	1	0	0	1	1	0	0	0	1
HBA	6	4	4	7	7	3	5	5	4	7	4	4	4	6
BBB[a]	Y[d]	n.a.	n.a.	Y[d]	Y[d]	n.a.	n.a.	n.a.	n.a.	N[b,e]	n.a.	n.a.	Y/N[b,e]	n.a.

inhibitors to maximize the ligand-protein interactions. For example, the amino group of triazines (**2–8**), thieno[3,2-*d*] pyrimidines (**13–15**), and conformationally restricted compounds **18, 22–35** is involved in an H-bond network with Asp2195 and Glu2195 in the binding affinity region. Compounds lacking a morpholine hinge region binding motif (**43–50**) usually have an HBD site employed for H-bonding interaction with the hinge region of mTOR (see Figure 7c for **43**). The investigated compounds **1–59** have a median HBD value of 1.4, in accordance to the approved CNS drugs. Among

ChemMedChem

Minireviews
doi.org/10.1002/cmdc.202100332

Chemistry Europe
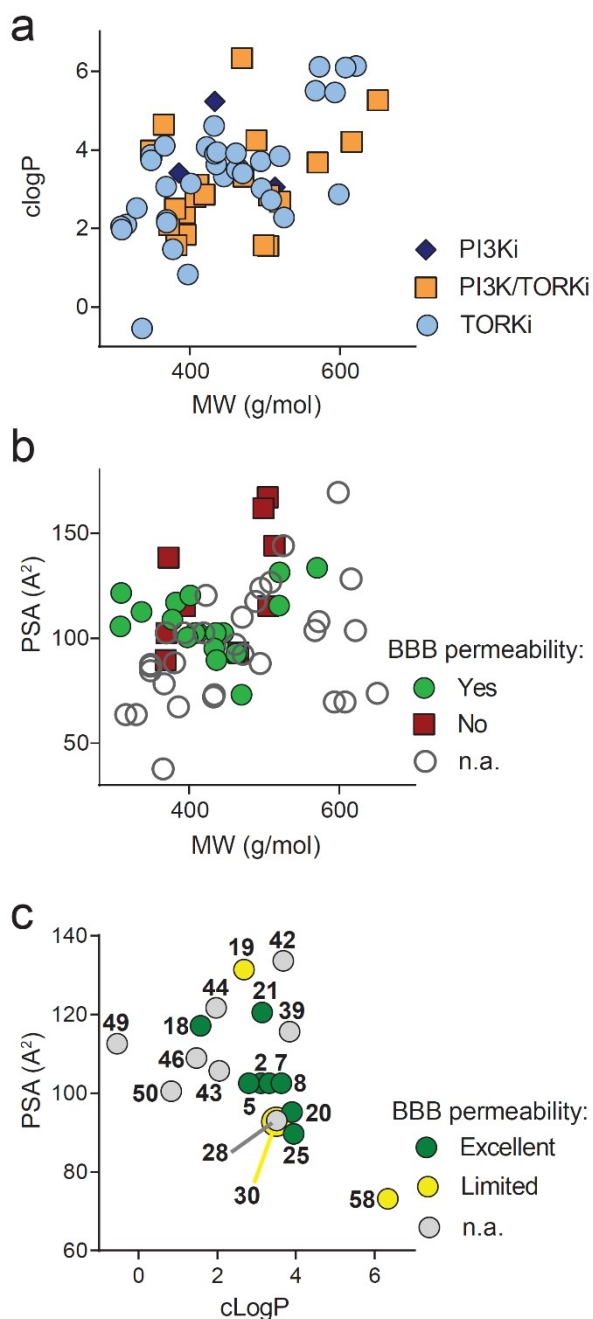European Chemical
Societies Publishing

Figure 9. Prolife of compounds **1–59** and brain permeability. a) cLogP values are plotted against MW values for TORKi (cyan full circles), dual PI3K/TORKi (orange full squares) and PI3Ki (blue full rhombus). b) PSA values plotted against MW for brain penetrant (green full circles) and non-BBB-penetrant (red full squares) inhibitors. When brain permeability has not been assessed, compounds are reported as gray empty circles (n.a. = not available). c) PSA values plotted against cLogP values for known brain penetrant compounds (green in Figure 9b). Compounds with excellent brain penetration (B/P ≥ 1, ER ≤ 1, green circles), limited brain access (B/P < 1, ER > 1, yellow circles), and compounds investigated in *in vivo* models of brain diseases or in clinical trials of glioblastoma, even though the brain distribution or transport-mediated efflux data are not available (n.a., gray full circles).

the brain penetrant mTOR inhibitors, triazines (**2**, **5**, **7**, **8**), tricyclic compounds (**18** and **25**), thiazolo[5,4-*d*]pyrimidine **21**, and purine **19** possessed one potential HBD group (Figure 7d).

Absence of an HBD was observed in compound **58**, displaying a limited BBB permeability.[82] Compound **43** is the only brain penetrant mTOR inhibitor with three HBD. It has been reported to significantly reduces tumor growth of glioblastoma (GBM) xenografts in mice,[88] however brain exposure and transporter-mediated efflux data are not available. In analogy to HBD, CNS drugs have usually a lower number of hydrogen bond acceptors (HBA) compared to that of non-CNS-permeable compounds.[89] For potential BBB permeability the following guidelines have been proposed: HBD < 3, HBA < 7, and total H-bonds < 8.[85] While the HBD count is in accordance to the guidelines for most mTOR brain permeable inhibitors, the median HBA value is 8.1. However, the number of hydrogen bond acceptors has been pointed out as the least important physicochemical predictor for BBB penetration.[81]

3.3. Brain Penetration for ATP-Competitive TORKi

Only a limited number of compounds targeting mTOR kinase has been investigated for their ability to cross the BBB (Figure 9b). Among them, no molecule bearing the thieno[3,2-*d*]pyrimidine scaffold (**12–15**) was found to reach the brain. The pan-PI3Ki **12** and the dual PI3K/mTOR inhibitors **13** and **15** poorly penetrate the BBB, showing $[brain]_u/[plasma]_u$ lower than 0.2 (0.05, 0.2 and 0.1, respectively). The brain penetration of compound **14** was also excluded considering the efflux measured in multidrug resistance gene (MDR1) cells. Although compounds **12** and **14** presented only one HBD (Figure 8d), they were P-gp substrates.[90] Pyrido[2,3-*d*]pyrimidine derivatives **29** and **30** showed a very limited brain penetration. **29** was reported as ABCB1 substrate and, accordingly, showed in-creased brain levels in Abcb1a/b$^{-/-}$;Abcg2$^{-/-}$ mice with respect to WT mice.[82] Even though **30** enhanced the radiosensitivity of GBM stem-like cells (GSCs) in a xenograft model,[91] detailed pharmacokinetic studies pointed out that **30** showed negligible brain permeability, reaching higher concentrations in plasma than in the brain (B/P: 0.04).[25a] Compound **28**, belonging to the same compounds class, is claimed as brain permeable TORKi since it showed efficacy in a traumatic brain injury model.[92] However, brain concentrations in WT animals or disease models are not reported. The dual PI3K/TORKi **55** is a substrate for P-gp and Bcrp, two efflux transporters at the BBB, leading to negligible brain concentration and hampering its applicability in the treatment of CNS disorders.[87] Another quinoline containing compound (**58**) is a substrate of Bcrp transporters, which limit its brain penetration to sub-therapeutic levels.[82] Brain exposure and transporter-mediated efflux data are missing for the claimed brain penetrant compounds **39**, **42–44**, **49–50** (Figure 9c, gray circles). The pyrazolopyrimidine **39** and the urea-substituted triazolopyrimidine **42** showed efficacy in mice bearing human glioblastoma astrocytoma (U87MG) xeno-graft models.[49,93] The 4-aminopyrazolo[3,4-*d*] pyrimidine **43** displayed antiproliferative effect in xenografted GBM cells in mice.[88] The follow-up compound **44** is currently in Phase I clinical trials for treatment of patients with recurrent glioblasto-ma [NCT02133183]. Compound **46** was also found to inhibit the

ChemMedChem

Minireviews
doi.org/10.1002/cmdc.202100332

Chemistry
Europe
European Chemical
Societies Publishing

growth of glioblastomas *in vitro* and *in vivo*,[94] and the derivatives **49** and **50** obtained through medicinal chemistry investigations are currently in clinical trials. The dihydropyrazino[2,3-*b*]pyrazin-2(1*H*)-one **49** has been included in a screening trial of innovative glioblastoma therapy [NCT02977780], while **50** has been assessed in different tumors including glioblastoma multiforme [NCT01177397].[95]

Chemical modifications on the triazine core led to inhibitors with specific targeting profiles and optimized brain penetration. While the dual PI3K/TORKi **4** showed negligible brain concentrations (B/P: 0.3, Figure 8d),[33] the dual PI3K/mTOR inhibitors **2**[32,96] and **5**[34] displayed excellent brain exposure (B/P: 1 and 1.67, Figure 8d and Figure 9c green circles). The highly selective TORKi **7** and **8** presented optimal brain penetration characterizing as candidates for the treatment of neurological disorders.[25a,b, 97] The purine-containing inhibitor **19** crossed the BBB and led to potent suppression of PI3K pathway biomarkers in the brain. It displayed efficacy and survival benefit in GBM models, even though it had a poor distribution to the brain (B/P: 0.1, Figure 8d and Figure 9c, yellow circle).[98] On the contrary, the purine-containing tricyclic compound **18** is capable of penetrating the BBB and demonstrated significant tumor growth inhibition in U87 glioblastoma xenograft mice.[42] **18** is currently investigated in a Phase II clinical trials for the treatment of patients with newly-diagnosed GBM [NCT03522298]. While the tricyclic compounds **22** and **24** did not cross the BBB,[28a] the conformationally restricted derivative **25** showed predicted BBB permeability in a MDCK-MDR1 permeability *in vitro* assay. **25** classified as the first pyrimido-pyrrolo-oxazine with potential application in the treatment of CNS disorders.[28b] The purine compound **20** and thiazolo[5,4-*d*]pyrimidine derivative **21** showed good permeability with no P-gp mediated efflux assessed using a MDCK-MDR1 assay. **21** presented desirable brain permeability in PK studies and efficacy in a mouse model of Tuberous Sclerosis Complex (TSC).[27]

4. Conclusions and Outlook

Dysregulation of mTOR signaling in cancer progression and neurological disorders has fueled the search for mTOR kinase inhibitors. The high structural similarity between the ATP-binding pocket of PI3K and mTOR kinase has hampered the development of highly selective TORKi. However, extensive medicinal chemistry campaigns allowed to pinpoint molecules that potently and selectively inhibit mTOR kinase. The chemical groups responsible for binding to the hinge region pocket or binding affinity region are herein analyzed. Altogether, essential insights on the chemical features responsible for mTOR selectivity and the physicochemical profile of TORKi have been generated. Even though a variety of scaffolds have been investigated for mTOR inhibition, high-throughput screenings and scaffold-hopping approaches could broaden the explored chemical space. In parallel to potency optimization, further medicinal chemistry efforts could still positively influence physicochemical properties. Controlling lipophilicity and avoid-

ing molecular obesity are essential to improve the success rate of drug discovery processes. Physicochemical descriptors, rather than potency alone, have to guide leads selection. For medicinal chemists interested in developing kinase inhibitors to treat CNS diseases, transporter-mediated efflux has to be limited. PSA and HBD are known to directly affect P-gp transport and should be carefully adjusted in the hit-to-lead phase. Synthetic chemistry modifications on kinase inhibitor scaffolds allow to fine-tune physicochemical properties, binding affinity, and pharmacological profiles. Thus, medicinal chemists possess the required tools to modulate brain exposure and develop optimized compounds for the treatment of CNS disorders.

Conflict of Interest

The authors declare no conflict of interest.

Keywords: mTOR inhibitors · chemical scaffolds · binding modes · physicochemical properties · BBB permeability

[1] a) M. P. Wymann, R. Schneiter, *Nat. Rev. Mol. Cell Biol.* **2008**, *9*, 162–176; b) H. Yang, D. G. Rudge, J. D. Koos, B. Vaidialingam, H. J. Yang, N. P. Pavletich, *Nature* **2013**, *497*, 217–223.

[2] a) M. Laplante, D. M. Sabatini, *Cell* **2012**, *149*, 274–293; b) J. Huang, B. D. Manning, *Biochem. J.* **2008**, *412*, 179–190.

[3] a) B. Magnuson, B. Ekim, D. C. Fingar, *Biochem. J.* **2012**, *441*, 1–21; b) Q. Yang, K. L. Guan, *Cell Res* **2007**, *17*, 666–681.

[4] a) D. D. Sarbassov, D. A. Guertin, S. M. Ali, D. M. Sabatini, *Science* **2005**, *307*, 1098–1101; b) M. P. Wymann, R. Marone, *Curr. Opin. Cell Biol.* **2005**, *17*, 141–149.

[5] D. A. Guertin, D. M. Sabatini, *Cancer Cell* **2007**, *12*, 9–22.

[6] R. Zoncu, A. Efeyan, D. M. Sabatini, *Nat. Rev. Mol. Cell Biol.* **2011**, *12*, 21–35.

[7] D. Fernandez, A. Perl, *Discov Med* **2010**, *9*, 173–178.

[8] J. R. Sampson, *Biochem. Soc. Trans.* **2009**, *37*, 259–264.

[9] S. C. Johnson, P. S. Rabinovitch, M. Kaeberlein, *Nature* **2013**, *493*, 338–345.

[10] B. Ravikumar, C. Vacher, Z. Berger, J. E. Davies, S. Luo, L. G. Oroz, F. Scaravilli, D. F. Easton, R. Duden, C. J. O'Kane, D. C. Rubinsztein, *Nat. Genet.* **2004**, *36*, 585–595.

[11] J. S. Talboom, R. Velazquez, S. Oddo, *NPJ Aging Mech. Dis.* **2015**, *1*, 15008.

[12] a) Z. Zhu, C. Yang, A. Iyaswamy, S. Krishnamoorthi, S. G. Sreenivasmurthy, J. Liu, Z. Wang, B. C.-K. Tong, J. Song, J. Lu, K.-H. Cheung, M. Li, *Int. J. Mol. Sci.* **2019**, *20*, 728; b) P. B. Crino, *Nat. Rev. Neurol.* **2016**, *12*, 379–392.

ChemMedChem

Minireviews
doi.org/10.1002/cmdc.202100332

Chemistry
Europe
European Chemical
Societies Publishing

[13] V. Veverka, T. Crabbe, I. Bird, G. Lennie, F. W. Muskett, R. J. Taylor, M. D. Carr, *Oncogene* **2008**, *27*, 585–595.

[14] J. Choi, J. Chen, S. L. Schreiber, J. Clardy, *Science* **1996**, *273*, 239–242.

[15] K. E. O'Reilly, F. Rojo, Q. B. She, D. Solit, G. B. Mills, D. Smith, H. Lane, F. Hofmann, D. J. Hicklin, D. L. Ludwig, J. Baselga, N. Rosen, *Cancer Res.* **2006**, *66*, 1500–1508.

[16] a) Y. Chen, X. Zhou, *Eur. J. Med. Chem.* **2020**, *208*, 112820; b) D. A. Sabbah, M. G. Brattain, H. Zhong, *Curr. Med. Chem.* **2011**, *18*, 5528–5544; c) Y. J. Zhang, Y. Duan, X. F. Zheng, *Drug Discovery Today* **2011**, *16*, 325–331.

[17] E. H. Walker, M. E. Pacold, O. Perisic, L. Stephens, P. T. Hawkins, M. P. Wymann, R. L. Williams, *Mol. Cell* **2000**, *6*, 909–919.

[18] a) M. P. Wymann, G. Bulgarelli-Leva, M. J. Zvelebil, L. Pirola, B. Vanhaese-broeck, M. D. Waterfield, G. Panayotou, *Mol. Cell. Biol.* **1996**, *16*, 1722–1733; b) G. J. Brunn, J. Williams, C. Sabers, G. Wiederrecht, J. C. Lawrence, Jr., R. T. Abraham, *EMBO J.* **1996**, *15*, 5256–5267.

[19] C. J. Vlahos, W. F. Matter, K. Y. Hui, R. F. Brown, *J. Biol. Chem.* **1994**, *269*, 5241–5248.

[20] Q. W. Fan, Z. A. Knight, D. D. Goldenberg, W. Yu, K. E. Mostov, D. Stokoe, K. M. Shokat, W. A. Weiss, *Cancer Cell* **2006**, *9*, 341–349.

[21] M. Hayakawa, H. Kaizawa, H. Moritomo, T. Koizumi, T. Ohishi, M. Yamano, M. Okada, M. Ohta, S. Tsukamoto, F. I. Raynaud, P. Workman, M. D. Waterfield, P. Parker, *Bioorg. Med. Chem. Lett.* **2007**, *17*, 2438–2442.

[22] a) K. Hara, Y. Maruki, X. Long, K. Yoshino, N. Oshiro, S. Hidayat, C. Tokunaga, J. Avruch, K. Yonezawa, *Cell* **2002**, *110*, 177–189; b) D. H. Kim, D. D. Sarbassov, S. M. Ali, J. E. King, R. R. Latek, H. Erdjument-Bromage, P. Tempst, D. M. Sabatini, *Cell* **2002**, *110*, 163–175; c) R. Loewith, E. Jacinto, S. Wullschleger, A. Lorberg, J. L. Crespo, D. Bonenfant, W. Oppliger, P. Jenoe, M. N. Hall, *Mol. Cell* **2002**, *10*, 457–468.

[23] a) M. Moll, P. W. Finn, L. E. Kavraki, *BMC Genomics* **2016**, *17 Suppl 4*, 431; b) D. Fabbro, S. W. Cowan-Jacob, H. Moebitz, *Br. J. Pharmacol.* **2015**, *172*, 2675–2700; c) J. J. Liao, *J. Med. Chem.* **2007**, *50*, 409–424.

[24] A. Zask, J. Kaplan, J. C. Verheijen, D. J. Richard, K. Curran, N. Brooijmans, E. M. Bennett, L. Toral-Barza, I. Hollander, S. Ayral-Kaloustian, K. Yu, *J. Med. Chem.* **2009**, *52*, 7942–7945.

[25] a) C. Borsari, E. Keles, D. Rageot, A. Treyer, T. Bohnacker, L. Bissegger, M. De Pascale, A. Melone, R. Sriramaratnam, F. Beaufils, M. Hamburger, P. Hebeisen, W. Löscher, D. Fabbro, P. Hillmann, M. P. Wymann, *J. Med. Chem.* **2020**, *63*, 13595–13617; b) D. Rageot, T. Bohnacker, A. Melone, J. B. Langlois, C. Borsari, P. Hillmann, A. M. Sele, F. Beaufils, M. Zvelebil, P. Hebeisen, W. Loscher, J. Burke, D. Fabbro, M. P. Wymann, *J. Med. Chem.* **2018**, *61*, 10084–10105; c) D. J. Richard, J. C. Verheijen, K. Yu, A. Zask, *Bioorg. Med. Chem. Lett.* **2010**, *20*, 2654–2657.

[26] J. C. Verheijen, K. Yu, L. Toral-Barza, I. Hollander, A. Zask, *Bioorg. Med. Chem. Lett.* **2010**, *20*, 375–379.

[27] S. Bonazzi, C. P. Goold, A. Gray, N. M. Thomsen, J. Nunez, R. G. Karki, A. Gorde, J. D. Biag, H. A. Malik, Y. Sun, G. Liang, D. Lubicka, S. Salas, N. Labbe-Giguere, E. P. Keaney, S. McTighe, S. Liu, L. Deng, G. Piizzi, F. Lombardo, D. Burdette, J.-C. Dodart, C. J. Wilson, S. Peukert, D. Curtis, L. G. Hamann, L. O. Murphy, *J. Med. Chem.* **2020**, *63*, 1068–1083.

[28] a) C. Borsari, D. Rageot, A. Dall'Asen, T. Bohnacker, A. Melone, A. M. Sele, E. Jackson, J.-B. Langlois, F. Beaufils, P. Hebeisen, D. Fabbro, P. Hillmann, M. P. Wymann, *J. Med. Chem.* **2019**, *62*, 8609–8630; b) C. Borsari, E. Keles, A. Treyer, M. De Pascale, P. Hebeisen, M. Hamburger, M. P. Wymann, *RSC Med. Chem.* **2021**, *12*, 579–583.

[29] K. G. Pike, K. Malagu, M. G. Hummersone, K. A. Menear, H. M. Duggan, S. Gomez, N. M. Martin, L. Ruston, S. L. Pass, M. Pass, *Bioorg. Med. Chem. Lett.* **2013**, *23*, 1212–1216.

[30] a) P. Nowak, D. C. Cole, N. Brooijmans, M. G. Bursavich, K. J. Curran, J. W. Ellingboe, J. J. Gibbons, I. Hollander, Y. Hu, J. Kaplan, D. J. Malwitz, L. Toral-Barza, J. C. Verheijen, A. Zask, W. G. Zhang, K. Yu, *J. Med. Chem.* **2009**, *52*, 7081–7089; b) J. C. Verheijen, D. J. Richard, K. Curran, J. Kaplan, M. Lefever, P. Nowak, D. J. Malwitz, N. Brooijmans, L. Toral-Barza, W. G. Zhang, J. Lucas, I. Hollander, S. Ayral-Kaloustian, T. S. Mansour, K. Yu, A. Zask, *J. Med. Chem.* **2009**, *52*, 8010–8024.

[31] a) T. Bohnacker, A. E. Prota, F. Beaufils, J. E. Burke, A. Melone, A. J. Inglis, D. Rageot, A. M. Sele, V. Cmiljanovic, N. Cmiljanovic, K. Bargsten, A. Aher, A. Akhmanova, J. F. Diaz, D. Fabbro, M. Zvelebil, R. L. Williams, M. O. Steinmetz, M. P. Wymann, *Nat. Commun.* **2017**, *8*, 14683; b) S. M. Maira, S. Pecchi, A. Huang, M. Burger, M. Knapp, D. Sterker, C. Schnell, D. Guthy, T. Nagel, M. Wiesmann, S. Brachmann, C. Fritsch, M. Dorsch, P. Chène, K. Shoemaker, A. De Pover, D. Menezes, G. Martiny-Baron, D. Fabbro, C. J. Wilson, R. Schlegel, F. Hofmann, C. García-Echeverría, W. R. Sellers, C. F. Voliva, *Mol. Cancer Ther.* **2012**, *11*, 317–328; c) S. M. Brachmann, J. Kleylein-Sohn, S. Gaulis, A. Kauffmann, M. J. Blommers, M.

Kazic-Legueux, L. Laborde, M. Hattenberger, F. Stauffer, J. Vaxelaire, V. Romanet, C. Henry, M. Murakami, D. A. Guthy, D. Sterker, S. Bergling, C. Wilson, T. Brümmendorf, C. Fritsch, C. Garcia-Echeverria, W. R. Sellers, F. Hofmann, S. M. Maira, *Mol. Cancer Ther.* **2012**, *11*, 1747–1757; d) M. T. Burger, S. Pecchi, A. Wagman, Z. J. Ni, M. Knapp, T. Hendrickson, G. Atallah, K. Pfister, Y. Zhang, S. Bartulis, K. Frazier, S. Ng, A. Smith, J. Verhagen, J. Haznedar, K. Huh, E. Iwanowicz, X. Xin, D. Menezes, H. Merritt, I. Lee, M. Wiesmann, S. Kaufman, K. Crawford, M. Chin, D. Bussiere, K. Shoemaker, I. Zaror, S. M. Maira, C. F. Voliva, *ACS Med. Chem. Lett.* **2011**, *2*, 774–779; e) S. Yaguchi, Y. Fukui, I. Koshimizu, H. Yoshimi, T. Matsuno, H. Gouda, S. Hirono, K. Yamazaki, T. Yamori, *J. Natl. Cancer Inst.* **2006**, *98*, 545–556; f) D. Kong, T. Yamori, *Cancer Sci.* **2007**, *98*, 1638–1642; g) G. W. Rewcastle, S. A. Gamage, J. U. Flanagan, R. Frederick, W. A. Denny, B. C. Baguley, P. Kestell, R. Singh, J. D. Kendall, E. S. Marshall, C. L. Lill, W. J. Lee, S. Kolekar, C. M. Buchanan, S. M. Jamieson, P. R. Shepherd, *J. Med. Chem.* **2011**, *54*, 7105–7126.

[32] F. Beaufils, N. Cmiljanovic, V. Cmiljanovic, T. Bohnacker, A. Melone, R. Marone, E. Jackson, X. Zhang, A. Sele, C. Borsari, J. Mestan, P. Hebeisen, P. Hillmann, B. Giese, M. Zvelebil, D. Fabbro, R. L. Williams, D. Rageot, M. P. Wymann, *J. Med. Chem.* **2017**, *60*, 7524–7538.

[33] C. Borsari, D. Rageot, F. Beaufils, T. Bohnacker, E. Keles, I. Buslov, A. Melone, A. M. Sele, P. Hebeisen, D. Fabbro, P. Hillmann, M. P. Wymann, *ACS Med. Chem. Lett.* **2019**, *10*, 1473–1479.

[34] D. Rageot, T. Bohnacker, E. Keles, J. A. McPhail, R. M. Hoffmann, A. Melone, C. Borsari, R. Sriramaratnam, A. M. Sele, F. Beaufils, P. Hebeisen, D. Fabbro, P. Hillmann, J. E. Burke, M. P. Wymann, *J. Med. Chem.* **2019**, *62*, 6241–6261.

[35] A. M. Venkatesan, C. M. Dehnhardt, E. Delos Santos, Z. Chen, O. Dos Santos, S. Ayral-Kaloustian, G. Khafizova, N. Brooijmans, R. Mallon, I. Hollander, L. Feldberg, J. Lucas, K. Yu, J. Gibbons, R. T. Abraham, I. Chaudhary, T. S. Mansour, *J. Med. Chem.* **2010**, *53*, 2636–2645.

[36] A. M. Venkatesan, Z. Chen, O. D. Santos, C. Dehnhardt, E. D. Santos, S. Ayral-Kaloustian, R. Mallon, I. Hollander, L. Feldberg, J. Lucas, K. Yu, I. Chaudhary, T. S. Mansour, *Bioorg. Med. Chem. Lett.* **2010**, *20*, 5869–5873.

[37] J. Kaplan, J. C. Verheijen, N. Brooijmans, L. Toral-Barza, I. Hollander, K. Yu, A. Zask, *Bioorg. Med. Chem. Lett.* **2010**, *20*, 640–643.

[38] A. J. Folkes, K. Ahmadi, W. K. Alderton, S. Alix, S. J. Baker, G. Box, I. S. Chuckowree, P. A. Clarke, P. Depledge, S. A. Eccles, L. S. Friedman, A. Hayes, T. C. Hancox, A. Kugendradas, L. Lensun, P. Moore, A. G. Olivero, J. Pang, S. Patel, G. H. Pergl-Wilson, F. I. Raynaud, A. Robson, N. Saghir, L. Salphati, S. Sohal, M. H. Ultsch, M. Valenti, H. J. Wallweber, N. C. Wan, C. Wiesmann, P. Workman, A. Zhyvoloup, M. J. Zvelebil, S. J. Shuttle-worth, *J. Med. Chem.* **2008**, *51*, 5522–5532.

[39] D. P. Sutherlin, D. Sampath, M. Berry, G. Castanedo, Z. Chang, I. Chuckowree, J. Dotson, A. Folkes, L. Friedman, R. Goldsmith, T. Heffron, L. Lee, J. Lesnick, C. Lewis, S. Mathieu, J. Nonomiya, A. Olivero, J. Pang, W. W. Prior, L. Salphati, S. Sideris, Q. Tian, V. Tsui, N. C. Wan, S. Wang, C. Wiesmann, S. Wong, B. Y. Zhu, *J. Med. Chem.* **2010**, *53*, 1086–1097.

[40] T. P. Heffron, M. Berry, G. Castanedo, C. Chang, I. Chuckowree, J. Dotson, A. Folkes, J. Gunzner, J. D. Lesnick, C. Lewis, S. Mathieu, J. Nonomiya, A. Olivero, J. Pang, D. Peterson, L. Salphati, D. Sampath, S. Sideris, D. P. Sutherlin, V. Tsui, N. C. Wan, S. Wang, S. Wong, B. Y. Zhu, *Bioorg. Med. Chem. Lett.* **2010**, *20*, 2408–2411.

[41] D. P. Sutherlin, L. Bao, M. Berry, G. Castanedo, I. Chuckowree, J. Dotson, A. Folks, L. Friedman, R. Goldsmith, J. Gunzner, T. Heffron, J. Lesnick, C. Lewis, S. Mathieu, J. Murray, J. Nonomiya, J. Pang, N. Pegg, W. W. Prior, L. Rouge, L. Salphati, D. Sampath, Q. Tian, V. Tsui, N. C. Wan, S. Wang, B. Wei, C. Wiesmann, P. Wu, B. Y. Zhu, A. Olivero, *J. Med. Chem.* **2011**, *54*, 7579–7587.

[42] T. P. Heffron, C. O. Ndubaku, L. Salphati, B. Alicke, J. Cheong, J. Drobnick, K. Edgar, S. E. Gould, L. B. Lee, J. D. Lesnick, C. Lewis, J. Nonomiya, J. Pang, E. G. Plise, S. Sideris, J. Wallin, L. Wang, X. Zhang, A. G. Olivero, *ACS Med. Chem. Lett.* **2016**, *7*, 351–356.

[43] T. Kashiyama, K. Oda, Y. Ikeda, Y. Shiose, K. Hirota, K. Inaba, C. Makii, R. Kurikawa, A. Miyasaka, T. Koso, T. Fukuda, M. Tanikawa, K. Shoji, K. Sone, T. Arimoto, O. Wada-Hiraike, K. Kawana, S. Nakagawa, K. Matsuda, F. McCormick, H. Aburatani, T. Yano, Y. Osuga, T. Fujii, *PLoS One* **2014**, *9*, e87220.

[44] K. Malagu, H. Duggan, K. Menear, M. Hummersone, S. Gomez, C. Bailey, P. Edwards, J. Drzewiecki, F. Leroux, M. J. Quesada, G. Hermann, S. Maine, C. A. Molyneaux, A. Le Gall, J. Pullen, I. Hickson, L. Smith, S. Maguire, N. Martin, G. Smith, M. Pass, *Bioorg. Med. Chem. Lett.* **2009**, *19*, 5950–5953.

[45] B. D. Guth, G. Rast, *Br. J. Pharmacol.* **2010**, *159*, 22–24.

ChemMedChem

Minireviews
doi.org/10.1002/cmdc.202100332

Chemistry
Europe
European Chemical
Societies Publishing

[46] C. M. Chresta, B. R. Davies, I. Hickson, T. Harding, S. Cosulich, S. E. Critchlow, J. P. Vincent, R. Ellston, D. Jones, P. Sini, D. James, Z. Howard, P. Dudley, G. Hughes, L. Smith, S. Maguire, M. Hummersone, K. Malagu, K. Menear, R. Jenkins, M. Jacobsen, G. C. Smith, S. Guichard, M. Pass, *Cancer Res.* **2010**, *70*, 288–298.

[47] K. Yu, L. Toral-Barza, C. Shi, W. G. Zhang, J. Lucas, B. Shor, J. Kim, J. Verheijen, K. Curran, D. J. Malwitz, D. C. Cole, J. Ellingboe, S. Ayral-Kaloustian, T. S. Mansour, J. J. Gibbons, R. T. Abraham, P. Nowak, A. Zask, *Cancer Res.* **2009**, *69*, 6232–6240.

[48] A. Zask, J. C. Verheijen, K. Curran, J. Kaplan, D. J. Richard, P. Nowak, D. J. Malwitz, N. Brooijmans, J. Bard, K. Svenson, J. Lucas, L. Toral-Barza, W. G. Zhang, I. Hollander, J. J. Gibbons, R. T. Abraham, S. Ayral-Kaloustian, T. S. Mansour, K. Yu, *J. Med. Chem.* **2009**, *52*, 5013–5016.

[49] K. Yu, C. Shi, L. Toral-Barza, J. Lucas, B. Shor, J. E. Kim, W. G. Zhang, R. Mahoney, C. Gaydos, L. Tardio, S. K. Kim, R. Conant, K. Curran, J. Kaplan, J. Verheijen, S. Ayral-Kaloustian, T. S. Mansour, R. T. Abraham, A. Zask, J. J. Gibbons, *Cancer Res.* **2010**, *70*, 621–631.

[50] D. J. Richard, J. C. Verheijen, K. Curran, J. Kaplan, L. Toral-Barza, I. Hollander, J. Lucas, K. Yu, A. Zask, *Bioorg. Med. Chem. Lett.* **2009**, *19*, 6830–6835.

[51] C. M. Dehnhardt, A. M. Venkatesan, E. Delos Santos, Z. Chen, O. Santos, S. Ayral-Kaloustian, N. Brooijmans, R. Mallon, I. Hollander, L. Feldberg, J. Lucas, I. Chaudhary, K. Yu, J. Gibbons, R. Abraham, T. S. Mansour, *J. Med. Chem.* **2010**, *53*, 798–810.

[52] Y. Liu, A. Bishop, L. Witucki, B. Kraybill, E. Shimizu, J. Tsien, J. Ubersax, J. Blethrow, D. O. Morgan, K. M. Shokat, *Chem. Biol.* **1999**, *6*, 671–678.

[53] B. Apsel, J. A. Blair, B. Gonzalez, T. M. Nazif, M. E. Feldman, B. Aizenstein, R. Hoffman, R. L. Williams, K. M. Shokat, Z. A. Knight, *Nat. Chem. Biol.* **2008**, *4*, 691–699.

[54] A. C. Hsieh, Y. Liu, M. P. Edlind, N. T. Ingolia, M. R. Janes, A. Sher, E. Y. Shi, C. R. Stumpf, C. Christensen, M. J. Bonham, S. Wang, P. Ren, M. Martin, K. Jessen, M. E. Feldman, J. S. Weissman, K. M. Shokat, C. Rommel, D. Ruggero, *Nature* **2012**, *485*, 55–61.

[55] D. S. Mortensen, S. M. Perrin-Ninkovic, R. Harris, B. G. Lee, G. Shevlin, M. Hickman, G. Khambatta, R. R. Bisonette, K. E. Fultz, S. Sankar, *Bioorg. Med. Chem. Lett.* **2011**, *21*, 6793–6799.

[56] D. S. Mortensen, S. M. Perrin-Ninkovic, G. Shevlin, J. Elsner, J. Zhao, B. Whitefield, L. Tehrani, J. Sapienza, J. R. Riggs, J. S. Parnes, P. Papa, G. Packard, B. G. Lee, R. Harris, M. Correa, S. Bahmanyar, S. J. Richardson, S. X. Peng, J. Leisten, G. Khambatta, M. Hickman, J. C. Gamez, R. R. Bisonette, J. Apuy, B. E. Cathers, S. S. Canan, M. F. Moghaddam, H. K. Raymon, P. Worland, R. K. Narla, K. E. Fultz, S. Sankar, *J. Med. Chem.* **2015**, *58*, 5599–5608.

[57] D. S. Mortensen, S. M. Perrin-Ninkovic, G. Shevlin, J. Zhao, G. Packard, S. Bahmanyar, M. Correa, J. Elsner, R. Harris, B. G. Lee, P. Papa, J. S. Parnes, J. R. Riggs, J. Sapienza, L. Tehrani, B. Whitefield, J. Apuy, R. R. Bisonette, J. C. Gamez, M. Hickman, G. Khambatta, J. Leisten, S. X. Peng, S. J. Richardson, B. E. Cathers, S. S. Canan, M. F. Moghaddam, H. K. Raymon, P. Worland, R. K. Narla, K. E. Fultz, S. Sankar, *J. Med. Chem.* **2015**, *58*, 5323–5333.

[58] a) Q. Liu, J. W. Chang, J. Wang, S. A. Kang, C. C. Thoreen, A. Markhard, W. Hur, J. Zhang, T. Sim, D. M. Sabatini, N. S. Gray, *J. Med. Chem.* **2010**, *53*, 7146–7155; b) Q. Liu, S. A. Kang, C. C. Thoreen, W. Hur, J. Wang, J. W. Chang, A. Markhard, J. Zhang, T. Sim, D. M. Sabatini, N. S. Gray, *Methods Mol. Biol.* **2012**, *821*, 447–460.

[59] Q. Liu, J. Wang, S. A. Kang, C. C. Thoreen, W. Hur, T. Ahmed, D. M. Sabatini, N. S. Gray, *J. Med. Chem.* **2011**, *54*, 1473–1480.

[60] S. Ding, N. S. Gray, X. Wu, Q. Ding, P. G. Schultz, *J. Am. Chem. Soc.* **2002**, *124*, 1594–1596.

[61] C. C. Thoreen, S. A. Kang, J. W. Chang, Q. Liu, J. Zhang, Y. Gao, L. J. Reichling, T. Sim, D. M. Sabatini, N. S. Gray, *J. Biol. Chem.* **2009**, *284*, 8023–8032.

[62] B. Markman, J. Tabernero, I. Krop, G. I. Shapiro, L. Siu, L. C. Chen, M. Mita, M. Melendez Cuero, S. Stutvoet, D. Birle, Ö. Anak, W. Hackl, J. Baselga, *Ann. Oncol.* **2012**, *23*, 2399–2408.

[63] S. D. Knight, N. D. Adams, J. L. Burgess, A. M. Chaudhari, M. G. Darcy, C. A. Donatelli, J. l. Luengo, K. A. Newlander, C. A. Parrish, L. H. Ridgers, M. A. Sarpong, S. J. Schmidt, G. S. Van Aller, J. D. Carson, M. A. Diamond, P. A. Elkins, C. M. Gardiner, E. Garver, S. A. Gilbert, R. R. Gontarek, J. R. Jackson, K. L. Kershner, L. Luo, K. Raha, C. S. Sherk, C. M. Sung, D. Sutton, P. J. Tummino, R. J. Wegrzyn, K. R. Auger, D. Dhanak, *ACS Med. Chem. Lett.* **2010**, *1*, 39–43.

[64] S. M. Maira, F. Stauffer, J. Brueggen, P. Furet, C. Schnell, C. Fritsch, S. Brachmann, P. Chène, A. De Pover, K. Schoemaker, D. Fabbro, D. Gabriel,

[65] a) W. J. Wang, L. M. Long, N. Yang, Q. Q. Zhang, W. J. Ji, J. H. Zhao, Z. H. Qin, Z. Wang, G. Chen, Z. Q. Liang, *Acta Pharm. Sin. B* **2013**, *34*, 681–690; b) R. Marone, D. Erhart, A. C. Mertz, T. Bohnacker, C. Schnell, V. Cmiljanovic, F. Stauffer, C. Garcia-Echeverria, B. Giese, S. M. Maira, M. P. Wymann, *Mol. Cancer Res.* **2009**, *7*, 601–613.

[66] F. Stauffer, S. M. Maira, P. Furet, C. García-Echeverría, *Bioorg. Med. Chem. Lett.* **2008**, *18*, 1027–1030.

[67] C. M. Hsu, P. M. Lin, Y. T. Tsai, M. S. Tsai, C. H. Tseng, S. F. Lin, M. Y. Yang, *Cell Death Dis.* **2018**, *4*, 57.

[68] R. Roskoski, Jr., *Pharmacol. Res.* **2021**, *165*, 105463.

[69] T. P. Heffron, *J. Med. Chem.* **2016**, *59*, 10030–10066.

[70] P. Tomasini, J. Egea, M. Souquet-Bressand, L. Greillier, F. Barlesi, *Ther Adv Respir Dis* **2019**, *13*, 1–11.

[71] R. Dziadziuszko, M. G. Krebs, F. De Braud, S. Siena, A. Drilon, R. C. Doebele, M. R. Patel, B. C. Cho, S. V. Liu, M. J. Ahn, C. H. Chiu, A. F. Farago, C. C. Lin, C. S. Karapetis, Y. C. Li, B. M. Day, D. Chen, T. R. Wilson, F. Barlesi, *J. Clin. Oncol.* **2021**, *39*, 1253–1263.

[72] N. U. Lin, V. Borges, C. Anders, R. K. Murthy, E. Paplomata, E. Hamilton, S. Hurvitz, S. Loi, A. Okines, V. Abramson, P. L. Bedard, M. Oliveira, V. Mueller, A. Zelnak, M. P. DiGiovanna, T. Bachelot, A. J. Chien, R. O'Regan, A. Wardley, A. Conlin, D. Cameron, L. Carey, G. Curigliano, K. Gelmon, S. Loibl, J. Mayor, S. McGoldrick, X. An, E. P. Winer, *J. Clin. Oncol.* **2020**, *38*, 2610–2619.

[73] a) D. A. Krueger, A. A. Wilfong, M. Mays, C. M. Talley, K. Agricola, C. Tudor, J. Capal, K. Holland-Bouley, D. N. Franz, *Neurology* **2016**, *87*, 2408–2415; b) D. A. Sabbah, R. Hajjo, S. K. Bardaweel, H. A. Zhong, *Expert Opin. Ther. Pat.* **2021**, 1–16.

[74] Z. Rankovic, *J. Med. Chem.* **2015**, *58*, 2584–2608.

[75] a) A. K. Ghose, T. Herbertz, R. L. Hudkins, B. D. Dorsey, J. P. Mallamo, *ACS Chem. Neurosci.* **2012**, *3*, 50–68; b) T. T. Wager, X. Hou, P. R. Verhoest, A. Villalobos, *ACS Chem. Neurosci.* **2010**, *1*, 435–449; c) T. T. Wager, R. Y. Chandrasekaran, X. Hou, M. D. Troutman, P. R. Verhoest, A. Villalobos, Y. Will, *ACS Chem. Neurosci.* **2010**, *1*, 420–434.

[76] C. A. Lipinski, F. Lombardo, B. W. Dominy, P. J. Feeney, *Adv. Drug Delivery Rev.* **2001**, *46*, 3–26.

[77] P. D. Leeson, B. Springthorpe, *Nat. Rev. Drug Discovery* **2007**, *6*, 881–890.

[78] H. van De Waterbeemd, D. A. Smith, K. Beaumont, D. K. Walker, *J. Med. Chem.* **2001**, *44*, 1313–1333.

[79] C. Hansch, J. P. Björkroth, A. Leo, *J. Pharm. Sci.* **1987**, *76*, 663–687.

[80] H. A. Zhong, V. Mashinson, T. A. Woolman, M. Zha, *Curr. Top. Med. Chem.* **2013**, *13*, 1290–1307.

[81] S. A. Hitchcock, L. D. Pennington, *J. Med. Chem.* **2006**, *49*, 7559–7583.

[82] F. Lin, M. C. de Gooijer, D. Hanekamp, G. Chandrasekaran, L. C. Buil, N. Thota, R. W. Sparidans, J. H. Beijnen, T. Würdinger, O. van Tellingen, *Clin. Cancer Res.* **2017**, *23*, 1286–1298.

[83] a) M. H. Abraham, *Eur. J. Med. Chem.* **2004**, *39*, 235–240; b) J. A. Gratton, M. H. Abraham, M. W. Bradbury, H. S. Chadha, *J. Pharm. Pharmacol.* **1997**, *49*, 1211–1216; c) H. van de Waterbeemd, G. Camenisch, G. Folkers, J. R. Chretien, O. A. Raevsky, *J. Drug Targeting* **1998**, *6*, 151–165.

[84] C. P. Tinworth, R. J. Young, *J. Med. Chem.* **2020**, *63*, 10091–10108.

[85] H. Pajouhesh, G. R. Lenz, *NeuroRx* **2005**, *2*, 541–553.

[86] M. Adenot, R. Lahana, *J. Chem. Inf. Comput. Sci.* **2004**, *44*, 239–248.

[87] S. Vaidhyanathan, B. Wilken-Resman, D. J. Ma, K. E. Parrish, R. K. Mittapalli, B. L. Carlson, J. N. Sarkaria, W. F. Elmquist, *J. Pharmacol. Exp. Ther.* **2015**, *356*, 251-259.

[88] B. Holmes, J. Lee, K. A. Landon, A. Benavides-Serrato, T. Bashir, M. E. Jung, A. Lichtenstein, J. Gera, *J. Biol. Chem.* **2016**, *291*, 14146–14159.

[89] P. D. Leeson, A. M. Davis, *J. Med. Chem.* **2004**, *47*, 6338–6348.

[90] T. P. Heffron, L. Salphati, B. Alicke, J. Cheong, J. Dotson, K. Edgar, R. Goldsmith, S. E. Gould, L. B. Lee, J. D. Lesnick, C. Lewis, C. Ndubaku, J. Nonomiya, A. G. Olivero, J. Pang, E. G. Plise, S. Sideris, S. Trapp, J. Wallin, L. Wang, X. Zhang, *J. Med. Chem.* **2012**, *55*, 8007–8020.

[91] J. Kahn, T. J. Hayman, M. Jamal, B. H. Rath, T. Kramp, K. Camphausen, P. J. Tofilon, *Neurooncology* **2014**, *16*, 29–37.

[92] Q. Lu, L. Gao, L. Huang, L. Ruan, J. Yang, W. Huang, Z. Li, Y. Zhang, K. Jin, Q. Zhuge, *J. Neuroinflammation* **2014**, *11*, 44.

[93] R. Mallon, I. Hollander, L. Feldberg, J. Lucas, V. Soloveva, A. Venkatesan, C. Dehnhardt, E. Delos Santos, Z. Chen, O. Dos Santos, S. Ayral-Kaloustian, J. Gibbons, *Mol. Cancer Ther.* **2010**, *9*, 976–984.

[94] B. Gini, C. Zanca, D. Guo, T. Matsutani, K. Masui, S. Ikegami, H. Yang, D. Nathanson, G. R. Villa, D. Shackelford, S. Zhu, K. Tanaka, I. Babic, D. Akhavan, K. Lin, A. Assuncao, Y. Gu, B. Bonetti, D. S. Mortensen, S. Xu, H. K. Raymon, W. K. Cavenee, F. B. Furnari, C. D. James, G. Kroemer, J. R.

ChemMedChem

Minireviews
doi.org/10.1002/cmdc.202100332

**Chemistry
Europe**
European Chemical
Societies Publishing

Heath, K. Hege, R. Chopra, T. F. Cloughesy, P. S. Mischel, *Clin. Cancer Res.* **2013**, *19*, 5722–5732.

[95] A. Varga, M. M. Mita, J. J. Wu, J. J. Nemunaitis, T. F. Cloughesy, P. S. Mischel, J. C. Bendell, K. C. Shih, L. G. Paz-Ares, A. Mahipal, J.-P. Delord, R. K. Kelley, J.-C. Soria, L. Wong, S. Xu, A. James, X. Wu, R. Chopra, K. Hege, P. N. Munster, *J. Clin. Oncol.* **2013**, *31*, 2606–2606.

[96] A. Wicki, N. Brown, A. Xyrafas, V. Bize, H. Hawle, S. Berardi, N. Cmiljanovic, V. Cmiljanovic, M. Stumm, S. Dimitrijevic, R. Herrmann, V. Pretre, R. Ritschard, A. Tzankov, V. Hess, A. Childs, C. Hierro, J. Rodon, D. Hess, M. Joerger, R. von Moos, C. Sessa, R. Kristeleit, *Eur. J. Cancer* **2018**, *96*, 6–16.

[97] a) E. Singer, C. Walter, D. Fabbro, D. Rageot, F. Beaufils, M. P. Wymann, N. Rischert, O. Riess, P. Hillmann, H. P. Nguyen, *Neuropharmacology* **2020**, *162*, 107812; b) W. Theilmann, B. Gericke, A. Schidlitzki, S. M. Muneeb Anjum, S. Borsdorf, T. Harries, S. L. Roberds, D. J. Aguiar, D.

Brunner, S. C. Leiser, D. Song, D. Fabbro, P. Hillmann, M. P. Wymann, W. Löscher, *Neuropharmacology* **2020**, *180*, 108297; c) C. Brandt, P. Hillmann, A. Noack, K. Römermann, L. A. Öhler, D. Rageot, F. Beaufils, A. Melone, A. M. Sele, M. P. Wymann, D. Fabbro, W. Löscher, *Neuropharmacology* **2018**, *140*, 107–120.

[98] D. Koul, S. Wang, S. Wu, N. Saito, S. Zheng, F. Gao, I. Kaul, M. Setoguchi, K. Nakayama, K. Koyama, Y. Shiose, E. P. Sulman, Y. Hirota, W. K. A. Yung, *Oncotarget* **2017**, *8*, 21741–21753.

MINIREVIEWS

Unraveling the profile of mTOR kinase inhibitors: Herein, we outline the chemical features driving potency and selectivity for mTOR over PI3Ks. Compounds covering a broad chemical space are examined, with particular emphasis on the modules engaging the different binding regions of the mTOR catalytic site. Physicochemical property analysis enabled to shed light on the descriptors influencing the brain penetration of ATP-competitive mTOR inhibitors.
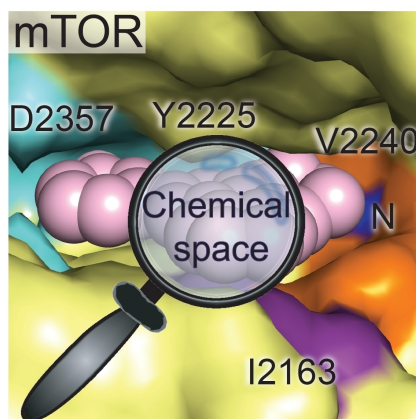
Dr. C. Borsari*, Dr. M. De Pascale, Prof. M. P. Wymann

1 – 17

Chemical and Structural Strategies to Selectively Target mTOR Kinase